Hepatic BSCL2 (Seipin) deficiency disrupts lipid droplet homeostasis and increases lipid metabolism via SCD1 activity

Mohamed Amine Lounis[1], Simon Lalonde[1], Sabri Ahmed Rial[1], Karl-F. Bergeron[1], Jessica C. Ralston[2], David M. Mutch[2], and Catherine Mounier[1]

[1] BioMed Research Center, Biological Sciences Department, University of Quebec in Montreal (UQÀM), Montreal, Quebec, Canada

[2] Department of Human Health & Nutritional Sciences, University of Guelph, Guelph, Ontario, Canada

Running title: Hepatic Seipin depletion increases SCD1 activity and LD formation

Corresponding author: Prof. Catherine Mounier, Département des sciences biologiques et centre de recherche BioMed, Université du Québec à Montréal, Case Postale 8888, Succursale Centre-ville, Montréal, QC, H3C 3P8, Canada. Phone: 1 (514) 987-3000 extension 8912. Fax: 1 (514) 987-4647. E-mail: mounier.catherine@uqam.ca

Key words: BSCL2, Seipin, lipid droplets, SCD1, lipogenesis, fatty acid uptake, insulin sensitivity

Abstract

Berardinelli-Seip congenital lipodystrophy (BSCL) is an autosomal recessive disorder. The more severe form, designated BSCL2, arises due to mutations in the *BSCL2* gene. Patients with BSCL2, as well as *Bscl2*$^{-/-}$ mice, have a near total absence of body fat, an organomegaly and develop metabolic disorders including insulin resistance and hepatic steatosis. The function of the Seipin (BSCL2) protein remains poorly understood. Several lines of evidence have indicated that Seipin may have distinct functions in adipose versus non-adipose cells. Here we present evidence that *BSCL2*/*Bscl2* plays a role in lipid droplet (LD) biogenesis and homeostasis in primary and cultured hepatocytes. Our results show that decreasing *BSCL2*/*Bscl2* expression in hepatocytes increases the number and size of LD, as well as the expression of genes implicated in their formation and stability. We also show that knocking down *SCD1* expression reverses the phenotype associated with Seipin deficiency. Interestingly, *BSCL2* knockdown induces SCD1 expression and activity, potentially leading to increased basal phosphorylation of proteins involved in the insulin signaling cascade, as well as further increasing fatty acid uptake and *de novo* lipogenesis. In conclusion, our results suggest that a hepatic *BSCL2*/*Bscl2* deficiency induces the increase and expansion of LD, potentially via increased SCD1 activity.

Abbreviations

Acetyl-CoA carboxylase (ACC*)*

1-acylglycerol-3-phosphate O-acyltransferases (AGPAT)

Adipose triglyceride lipase (ATGL)

activating transcription factor-6 (ATF6)

analysis of variance (ANOVA)

Berardinelli-Seip congenital lipodystrophy (BSCL)

bovine serum albumin (BSA)

cell death-inducing DFFA-like effector a (CIDEA)

cholesteryl esters (CE)

diacylglycerol (DAG)

double-stranded RNA-dependent protein kinase-like ER kinase (PERK)

endoplasmic reticulum (ER)

Fatty acid synthase (FAS)

Fond de Recherche du Québec-Nature et Technologie (FRQNT)

glucose-6-phosphatase catalytic subunit (G6pc)

glucokinase (Gck)

glucose-regulated protein 78 (GRP78)

glucose tolerance test (GTT)

glyceraldehyde-3-phosphate dehydrogenase (GAPDH)

hypoxanthine phosphoribosyltransferase 1 (HPRT1)

inositol-requiring transmembrane kinase and endonuclease 1a (IRE1a)

insulin receptor substrate (IRS)

insulin tolerance test (ITT)

knockout (KO)

lipid droplet (LD)

mechanistic target of rapamycin (mTOR)

monounsaturated fatty acids (MUFA)

National Science and Engineering Research Council of Canada (NSERC)

non-alcoholic steatohepatitis (NASH)

peroxisome proliferator activated receptor (PPAR)

perilipin 5 (PLIN5*)*

Phosphoenolpyruvate carboxykinase (Pepck)

phosphate-buffered saline (PBS)

phospholipids (PL)

saturated fatty acids (SFA)

Sterol regulatory element binding protein-1c (SREBP-1c)

stearoyl-CoA desaturase 1 (SCD1)

triacylglycerol (TAG)

unesterified fatty acids (FFA)

unfolded protein response (UPR)

wildtype (WT)

Introduction

Berardinelli-Seip syndrome is an autosomal form of congenital generalized lipodystrophy [1] identified by Berardinelli [2] from Brazil and Seip from Scandinavia [3]. The most severe form of this disorder is Berardinelli-Seip congenital lipodystrophy type 2 (BSCL2), which is due to a loss of function of the *BSCL2* gene [4-6]. This disorder is characterized by generalized lipodystrophy, insulin resistance, hypertriglyceridemia and severe hepatic steatosis [4-6]. In order to understand the function of the Seipin (BSCL2) protein, several groups have generated *Bscl2* knockout mice (*Bscl2*$^{-/-}$) [7-9]. Besides the generalized lipodystrophic phenotype, *Bscl2*$^{-/-}$ mice develop most of the metabolic complications observed in patients carrying *BSCL2* null mutations. Organomegaly has been reported in two *Bscl2*$^{-/-}$ lines, with an increased size of liver, kidneys, intestine, epididymis, heart and spleen. *Bscl2*$^{-/-}$ mice also suffer from massive hepatic steatosis, a decrease in energy expenditure, hyperglycemia, severe glucose intolerance, and insulin resistance [7-9]. *Bscl2*$^{-/-}$ mice revealed a critical role for Seipin in adipocyte maturation [9, 10]. It appears that loss of *Bscl2* does not inhibit adipogenesis, but rather abrogates triacylglycerol (TAG) synthesis, thereby preventing the full maturation of adipocytes and subsequently leading to lipodystrophy [11]. The role of Seipin in non-adipose tissues remains unclear. Humans carrying *BSCL2* mutations, as well as *Bscl2*$^{-/-}$ mice, develop severe hepatic steatosis associated with hepatic failure. Ectopic storage of lipids in the form of intracellular droplets within hepatocytes induces lipotoxicity, which is associated with severe pathological conditions including insulin resistance, pancreatic β-cell failure and non-alcoholic steatohepatitis (NASH), as well as hepatic inflammation [12-14]. In the absence of a functional Seipin protein, hepatic steatosis may be a consequence of a cell-intrinsic effect or a cell-extrinsic effect such as the disappearance of adipose tissue [15]. *Bscl2* deficiency also has an intriguing impact on insulin sensitivity. Two recently published studies based on insulin and glucose tolerance tests (ITT and GTT, respectively) demonstrated that *Bscl2*$^{-/-}$ mice are insulin resistant [7, 8]. In contrast, another group showed insulin hypersensitivity in fasting *Bscl2*$^{-/-}$ mice, suggesting that under specific conditions these mice are not insulin resistant [16].

TAG are stored in the cell within lipid droplets (LD). Several studies have provided evidence that Seipin plays an evolutionarily conserved role in the biogenesis of LD in various models and tissues, including LD formation and homeostasis [8, 17-22]. Fei and colleagues suggested that the absence of *Bscl2* increases the level of neutral lipids in yeast, leading to the formation of supersized LD [19, 23, 24]. Knocking down *BSCL2* in HeLa and NIH/3T3 cells significantly increases TAG synthesis and storage in LD, whereas its over-expression has the opposite effect [25]. In the salivary gland of *Drosophila, Seipin* deficiency promotes the accumulation of LD by increasing diacylglycerol (DAG) and TAG synthesis and storage [26]. In hepatic AML-12 cells, the overexpression of *Bscl2* inhibits LD formation [27]. Hence, low Seipin levels are systematically associated with increased TAG synthesis and/or LD formation. However, the particular mechanism by which Seipin participates in LD biogenesis remains unclear.

LD formation begins within ER membrane leaflets [28, 29]. Recently, Seipin was hypothesized to be a central scaffold protein within the ER [30]. In adipocytes, Seipin interacts with the adaptor protein 14-3-3β and may influence cytoskeletal remodeling [31]. Seipin also interacts with SERCA, an ER Ca^{2+}-ATPase regulating lipid storage in adipocytes [32]. Finally, Talukder and collaborators demonstrated that Seipin can form a complex with AGPAT2 and LPIN1 (Lipin-1) to modulate ER-based lipogenesis and adipogenesis [30]. Several reports have implicated the disruption of ER homeostasis, or ER stress, in the development of hepatic steatosis [33-38]. Any event that leads to a disruption of ER homeostasis, such as excessive protein synthesis, an accumulation of misfolded protein or a change in calcium levels will induce an unfolded protein response (UPR) [38-40]. In mammalians cells, the UPR is mediated by three ER proteins: 1) the inositol-requiring transmembrane kinase and endonuclease 1a (IRE1a), 2) the double-stranded RNA (dsRNA)-dependent protein kinase-like ER kinase (PERK), and 3) the activating transcription factor-6 (ATF6) [41]. In physiologically normal conditions, these proteins are kept inactive through their association with the ER chaperone glucose-regulated protein 78 (GRP78)/ immunoglobulin-heavy-chain-binding protein. Following the induction of ER stress, GRP78 releases the three UPR proteins in order to manage the accumulation of unfolded proteins, resulting in the activation of PERK, IRE1a, and ATF6 [38].

The present study aimed to analyze the effect of Seipin deficiency on the formation and homeostasis of LD in cultured hepatocytes. *Bscl2*/*BSCL2* knockdown modified the quantity and morphology of LD, and affected their growth and aggregation. This was associated with an induction of SCD1 expression and activity, as reflected by an increase in the ratio of monounsaturated fatty acids to saturated fatty acids (MUFA/SFA). In these conditions, fatty acid uptake and *de novo* lipogenesis were also activated. In addition, we showed that lowering Seipin levels in hepatocytes increased basal phosphorylation of insulin signaling proteins. Our data also revealed that the Seipin deficiency phenotype could be reversed with a *SCD1* knockdown. Finally, concomitant to increased lipid storage, *BSCL2*/*Bscl2* knockdown triggered an activation of ER stress in hepatocytes.

Materials and Methods

Bscl2 knockout samples

Liver samples and whole cell extracts (mRNA and proteins) from *Bscl2*$^{-/-}$ mice were a generous gift from Dr. Jocelyne Magré (INSERM, University of Nantes, France) and Dr. Xiaoqin Ye (University of Georgia, USA). Mice were housed and monitored in accordance with protocols approved by their local animal care committees. Fasted (for 24h, beginning and ending in the morning, during the light period of the light/dark cycle) and non-fasted (fed) mice were used to test different physiological conditions (basal versus nutrient-rich, respectively) under a standard low fat diet [8].

Cell culture and transfection

Primary hepatocytes were isolated from 3-month-old (125g) male Sprague Dawley rats (Harlan Laboratories) using a collagenase perfusion protocol [42, 43]. Harvested hepatocytes were plated on collagen-coated 12-well plates in DMEM/F12 medium (1:1; Wisent) containing 10% fetal bovine serum (Hyclone Laboratories) and 1% penicillin-streptomycin-amphotericin B (Thermo Fisher Scientific). Following an overnight incubation (37°C, 5% CO_2), cells were washed with 1x phosphate-buffered saline (PBS) and serum-free medium was added for 24h before further treatments. The University of Quebec at Montreal's Animal Care Committee (CIPA) approved all experimental protocols.

HepG2 human hepatocyte cells (ATCC) were cultured in EMEM medium (Wisent) supplemented with 10% fetal bovine serum, 100U/ml penicillin and 100µg/ml streptomycin (Thermo Fisher Scientific). At confluence, serum-free medium without antibiotics was applied for 24h.

After 24h in serum-free medium, HepG2 cells and primary rat hepatocytes were transfected overnight using the DharmaFECT4 reagent with either negative control No. 1 (CTRL), *BSCL2* and/or *SCD1* (in HepG2 cells), or *Bscl2* (in primary rat hepatocytes) Silencer Select siRNA(s) according to the manufacturer's instructions (#4390843,

#4392420 / s25559, #4390824 / s12503 and #4390771 / s167880; Thermo Fisher Scientific). The next day, cells were treated for 24h with 100µM oleate (2 mol/mol BSA; Sigma-Aldrich) or 50µM BSA (equivalent to control condition). For insulin sensitivity experiments, cells were stimulated for 10min with 100nM insulin following siRNA transfection.

Lipid droplet imaging

After siRNA transfection and incubation of cells with 100µM oleate, HepG2 cells and primary rat hepatocytes were washed three times with ice-cold 1x PBS and fixed in 4% paraformaldehyde for 30min. LD were stained for 10min with Bodipy 493/503 (1µg/ml; Thermo Fisher Scientific). Fluorescence was visualized with a Nikon A1 confocal microscope. Each measurement of LD size and LD number per cell was obtained from over 240 cells (6 images per condition with at least 40 cells per image) using *Image J* software. Only particles falling in the 1 to 50µm range were considered for analysis.

For time-lapse confocal microscopy, siRNA-transfected HepG2 cells were incubated with 100µM oleate in the presence of 1µg/ml Bodipy 493/502 overnight at 37°C under 5% CO_2. Z-stacks were acquired every 10min over a 10h period using a Nikon A1 confocal microscope in order to image whole cells. Video frames were analyzed with *Image J* software using the threshold function to outline Bodipy-labelled LD.

Quantitative reverse transcription-polymerase chain reaction (qRT-PCR)

Total RNA from tissues and cells were extracted using the Trizol reagent (Thermo Fisher Scientific), according to manufacturer's instructions. Total RNA (500ng) was reverse transcribed (SuperScript II reverse transcriptase; Thermo Fisher Scientific) and quantitative real-time PCR was performed using SYBR Green I Master Mix on a LightCycler 480 Real-Time PCR System (Roche Applied Science). Results are represented as arbitrary units indicating relative expressions based on the comparative Ct (ΔΔCt) method. Data were normalized using housekeeping genes *Cyclophilin A* (for mouse tissue) or *Hypoxanthine phosphoribosyltransferase 1* (*HPRT1*; for human cells),

and presented as fold changes relative to control samples.

Immunohistochemistry

HepG2 cells were fixed on slides with 4% paraformaldehyde for 30min at RT. Fixed HepG2 cells, were blocked for one hour in 1x PBS containing 1.5% normal goat serum. Samples were incubated with anti-Seipin primary antibody (Santa Cruz Biotechnology, clone L-16; 1:50) overnight at 4°C before using the ImmunoCruz goat ABC staining system (Santa Cruz Biotechnology). Nuclei were stained with Hematoxylin Gill no°3 (Sigma-Aldrich).

Immunofluorescence

To study SCD1 and Seipin protein colocalization, HepG2 cells were fixed with 4% paraformaldehyde and permeabilized with 0.1% Triton X-100. Cells were washed with PBS, blocked with 3% BSA in Tris-buffered saline containing 1% Triton X-100 and then incubated with anti-SCD1 (Abcam; mouse primary 1:200) and anti-Seipin (Santa Cruz Biotechnology, clone L-16; rabbit primary 1:50). Cells were washed with PBS and incubated with anti-mouse Alexa Fluor 488 and anti-rabbit Alexa Fluor 647 (Abcam; goat secondary 1:1000). The cells were washed with PBS and images acquired using a Nikon A1 confocal microscope fitted with a 100x oil immersion lens. For colocalization analysis, Pearson's *r* and Spearman's *p* correlation coefficients were obtained from over 200 cells (10 images with at least 20 cells per image) using the Coloc2 analysis plugin in ImageJ software.

Immunoblot analysis

After siRNA transfection and incubation with 100µM oleate, cells were lysed in RIPA buffer supplemented with cOmplete protease inhibitors and phosphatase inhibitor cocktail 3 (Sigma-Aldrich). Proteins were denatured at 95°C for 5min, 30µg protein/lane was loaded onto SDS-PAGE and immunoblot analyses were carried out using the antibodies listed in **Table 1**. Protein extracts from rat testis, adipose tissue and primary

hepatocytes, mouse livers as well as human hepatocyte-hepatocarcinoma HepG2 cells were probed with the anti-Seipin antibody (Santa Cruz Biotechnology, clone L-16; 1:50). *Image J* software was used to quantify band intensity.

Lipid extraction and quantification using gas chromatography

Cells transfected with siRNA (as well as corresponding controls) were trypsinized for 5min, collected and spun at 1200rpm for 5min to pellet hepatocytes. HepG2 cell pellets were washed in 1x PBS. Lipid extractions were conducted using previously described protocols [44, 45]. Samples were analyzed using a 7890B gas chromatography system (Agilent Technologies) with a flame ionization detector, and samples were separated on a J&W DBFFAP fused-silica capillary column (15m, 0.1μm film thickness, 0.1mm i.d.; Agilent Technologies). Fatty acid peaks were identified by comparison with retention times of fatty acid methyl ester standards. To estimate SCD1 activity, we calculated the product-to-precursor fatty acid ratio (i.e., 18:1n9/18:0 and 16:1n7/16:0), as previously reported [46, 47]. Fatty acid data were normalized to protein concentrations for each treatment condition and reported as μg fatty acid per μg/μl protein.

Fatty acid uptake

Uptake of [^{3}H]oleate was measured in confluent HepG2 cells and rat primary hepatocytes as previously described [48, 49]. Briefly, 0.68μCi of [9,10-^{3}H]oleic acid (54.6 Ci/mmol; Perkin Elmer) was mixed with 50μM of non-radioactive oleate (Sigma-Aldrich) and dissolved in a 173μM BSA solution free of fatty acids. Cells were incubated with this oleate/BSA solution for 10min at 37°C. Uptake was stopped by removal of the oleate/BSA solution followed by the addition of ice-cold 1x PBS (5ml) containing 200μM of phloretin and 0.1% BSA (wt/v). After a 2min incubation, cells were washed six times with ice-cold 1x PBS. Cells were then lysed with 2M NaOH and aliquots of the lysate were used for protein concentration and radioactivity measurements. Radioactivity was measured in a TRI Carb 2800TR liquid scintillation counter after the addition of 10ml Ultima-Gold (Perkin Elmer). Data were presented as number of counts per minute

(CPM) of [^{3}H] per µg of protein.

De novo lipogenesis

De novo lipogenesis was evaluated by measuring the incorporation of [^{14}C]acetate into lipids, as described previously [44, 50, 51]. Briefly, post-transfection cells were incubated with 1µCi of [1,2-^{14}C]acetic acid (54.3 Ci/mol; Perkin Elmer) for 4h. Cells were then suspended in 200µl 1x PBS and total cellular lipids were extracted in chloroform/methanol (2:1, v/v). The lipid extract was dried under nitrogen and reconstituted in 100µl hexane. Radiolabeled lipids were separated by thin layer chromatography on silica-coated plates using a hexane/diethyl-ether/acetic acid solution (80:20:1, v/v) as a developing solvent [44, 50, 51]. Lipids were visualized by exposure to iodine vapors and the bands corresponding to authentic lipid standards (FFA, TAG, DAG, CE, and PL) were scraped into separate vials. Radioactivity was measured and data presented as CPM of [^{14}C] per µg of protein.

Statistical analysis

When evaluating statistical significance, we used a Student's t-test (two-tailed) to compare two groups and a two-way analysis of variance (ANOVA) when more than one factor was evaluated. A $p<0.05$ was considered statistically significant. Unless specified otherwise, data are presented as mean ± SD.

Results

Seipin is expressed in hepatocytes

Since Seipin as yet to be shown to play a cell autonomous role in the liver, our first aim was to confirm the presence of the Seipin protein in the various hepatic models used in this study. To this end, we performed antibody-based analyses in HepG2 cells (a human hepatocyte-hepatocarcinoma cell line) as well as in rat primary hepatocytes. The testis, a tissue known to express Seipin [52], was used as positive control. An anti-Seipin antibody (**Table 1**), detected a band of ~67kD in the rat testis and a major band at ~60kD in the rat adipose tissue, in agreement with previous observations [52]. Primary rat hepatocytes also showed a ~60kD band while HepG2 cells displayed a slightly higher band (~61kD), presumably reflecting the fact that human Seipin is 33 amino acids longer. The detected levels of Seipin were lower in adipocytes and hepatocytes compared to testis (**Fig.1A, *left panels***). A ~60kD band detected in liver extracts of WT mice was absent in liver extracts of *Bscl2*$^{-/-}$ mice (**Fig.1A, *right panels***), confirming antibody specificity. We used immunohistochemistry to expand and confirm these results. The Seipin protein was concentrated in the perinuclear space of HepG2 cells, a pattern consistent with ER localization (**Fig.1B**).

BSCL2 knockdown alters lipid droplet morphology and size

To evaluate the role of Seipin *in vitro*, primary rat hepatocytes and HepG2 cells were transfected with a siRNA designed to knockdown *Bscl2*/*BSCL2*. This approach decreased Seipin protein levels to 54% and 36% in HepG2 cells (**Fig.1C, *left panels***) and primary rat hepatocytes (**Fig.1C, *right panels***), respectively. Oleate treatment was then used to induce LD formation, increasing both number and size of the organelle (**Fig.2A**). Inhibition of *Bscl2*/*BSCL2* expression increased the number (80% more) and the size (150% larger) of LD, irrespective of the presence of oleate, in both rat primary hepatocytes and HepG2 cells (**Fig.2A**). Live imaging of Seipin-deficient HepG2 cells showed greater LD clustering with at least partial LD fusion, resulting in aggregates of

abnormal morphology, and suggested increased LD persistence (**Fig.2B**). We analyzed mRNA expression levels of key genes implicated in LD homeostasis. In both HepG2 cells and the liver of *Bscl2*$^{-/-}$ mice (**Fig.3**), a Seipin deficiency was associated with increased expression of *Plin5*/*PLIN5* and *Cidea*/*CIDEA*; genes involved in LD formation and stability, respectively [53, 54]. In contrast, a decrease in *Atgl*/*ATGL* expression, a gene known to be involved in lipolysis [55-57], was observed in HepG2 cells and the liver of fasted *Bscl2*$^{-/-}$ mice, but not in fed mice. Together, our data suggest that lowering Seipin levels in hepatocytes increased LD biogenesis.

Alteration of lipid droplet homoeostasis following *BSCL2* knockdown is concomitant with changes in lipid metabolism

In order to better understand the mechanism underlying the observed increase in LD formation and expansion in Seipin-deficient cells (**Fig.2**), we evaluated fatty acid uptake by [^{3}H]oleate incorporation into HepG2 cells and primary rat hepatocytes following siRNA transfection. *Bscl2*/*BSCL2* knockdown caused an increase in fatty acid uptake in both HepG2 cells and primary rat hepatocytes (40%; **Fig.4A**). In siRNA-transfected HepG2 cells, elevated fatty acid uptake was associated with increased levels of the PPARγ transcription factor (40%; **Fig.4B, *top panel***) and at least one of its direct targets, the translocase CD36 implicated in fatty acid transport [58] (80%; **Fig.4B, *middle panel***). It has recently been shown that Seipin can have an effect on PPARγ nuclear localization and activity through an interaction with the TAG synthesis enzyme AGPAT2 [30]. We therefore investigated AGPAT2 levels in our siRNA-transfected cells. Interestingly, Seipin deficiency led to increased expression of AGPAT2 (40%; **Fig.4B, *bottom panel***).

To determine if *de novo* lipogenesis was also affected by diminished Seipin levels, we measured [^{14}C]acetate incorporation into lipids of siRNA-transfected hepatic cells. A 25% increase in the synthesis of total lipids was observed in HepG2 cells transfected with *BSCL2* siRNA (**Fig.5A, *top panel***). This higher overall synthesis was primarily due to increased synthesis of TAG and DAG (22% and 28% respectively; **Fig.5A, *bottom panels***). No difference was observed in the other lipid fractions examined, such as free fatty acids, ceramides and cholesterol esters (*data not shown*). In siRNA-transfected

HepG2 cells, elevated *de novo* lipogenesis was also associated with increased expression of several lipogenic enzymes such as ACC, FAS and SCD1, as well as the transcription factor SREBP-1c (**Fig.5B**). In addition, an increase in mature SREBP-1c protein levels was observed in the liver of *Bscl2*$^{-/-}$ mice (**Fig.5C**). Interestingly, we also showed a decrease in the expression of proteins implicated in lipolysis [55-57] and β-oxidation [59, 60] (ATGL and PPARα, respectively) (**Fig.5B, *bottom panels***), suggesting that inhibition of β-oxidation may contribute to the LD alterations observed in Seipin-deficient cells.

Seipin and SCD1 have opposing effect on LD formation and lipid synthesis

We showed an induction of SCD1 expression in Seipin-deficient cultured hepatocytes (**Fig.5B**). A similar result was reported in the liver of *Bscl2*$^{-/-}$ mice [8]. The mostly perinuclear pattern of expression observed for both SCD1 and Seipin is consistent with the expected localization of these two ER-resident proteins. We determined that SCD1 and Seipin colocalize in HepG2 cells (Pearson's *r* value: 0.63, Spearman's *p* value: 0.47; **Fig.6A**), hinting to a possible functional relationship between these two proteins. We therefore tested the effect of *SCD1* deficiency in HepG2 cells using a validated siRNA (**Fig.6B**). Co-transfection of *SCD1* and *BSCL2* siRNA rescued the Seipin deficiency phenotype, i.e., the number and size of LD was close to normal when compared to cells transfected with *BSCL2* siRNA alone, irrespective of the presence or absence of oleate (**Fig.6C**). The increase in fatty acid uptake (**Fig.6D**) and *de novo* lipogenesis (**Fig.6E**) observed in Seipin-deficient HepG2 cells was also lost when cells were co-transfected with *SCD1* and *BSCL2* siRNA. Co-transfected cells exhibited a low lipid uptake and synthesis profile closer to that of cells transfected with *SCD1* siRNA alone. In a similar fashion, we found that the MUFA/SFA ratio is higher in Seipin-deficient hepatocytes compared to non-transfected control HepG2 cells, whereas it tended to be lower in SCD1-deficient or co-transfected cells (**Fig.6F**). Together, these observations show that Seipin and SCD1 have opposing effects on LD formation and lipid synthesis, and suggest that Seipin's effect on hepatic lipid synthesis/accumulation is mediated by SCD1.

Seipin deficiency increases basal phosphorylation of insulin-signaling proteins

General insulin resistance and hyperglycemia are characteristic of patients with BSCL2 [5, 17, 61], as well as *Bscl2*$^{-/-}$ mice [7-9]. We therefore evaluated the expression level and the phosphorylation state of key proteins involved in the insulin-signaling cascade. Seipin deficiency was associated with increased phosphorylation of AKT (both Ser473 and Thr308 sites), ERK1/2, mTOR and P70S6K in HepG2 cells stimulated or not by insulin (**Fig.7A**). The levels of AKT (Ser473) and IRS1 (Tyr612) phosphorylation were also increased in liver extracts of *Bscl2*$^{-/-}$ mice (**Fig.7B**). In accordance with an increase in the phosphorylation of insulin-signaling proteins, we noted that, in *Bscl2*$^{-/-}$ mice, the expression of glucose metabolism markers such as *Gck* was increased while *G6pc* expression was decreased. Unexpectedly, *Pepck* expression was increased (**Fig.7C**).

We then analyzed the effect of *BSCL2* knockdown on physiological responses activated by insulin. We stimulated siRNA-transfected rat primary hepatocytes with insulin and measured both fatty acid uptake and *de novo* lipogenesis. In accordance with initial observations (**Figs.4&5**), Seipin deficiency increased both fatty acid uptake and lipogenesis. However, the presence of insulin further stimulated fatty acid uptake (25% compared to *BSCL2* siRNA-transfected cells without insulin) (**Fig.7D**) and *de novo* lipogenesis (35% total lipids, compared to *BSCL2* siRNA-transfected cells without insulin) (**Fig.7E**). As previously observed (**Fig.5A**), increased *de novo* lipogenesis primarily stemmed from increased TAG and DAG synthesis (**Fig.7E**), as the levels of others lipid classes did not vary (*data not shown*). These data suggest that in cases of Seipin deficiency, hepatic lipid uptake and synthesis as well as gluconeogenesis are increased, probably aggravating the BSCL2 phenotype and contributing to hepatic dysfunction.

Seipin deficiency increases the expression of ER stress markers

ER stress and the unfolded protein response (UPR) are critically involved in the initiation of many diseases, such as the metabolic syndrome [40, 62, 63]. In addition, this pathway has been reported to play an important role in LD formation and lipogenesis promotion in the liver [39, 64]. To determine if Seipin deficiency could induce ER stress, we measured the mRNA levels of key genes implicated in this process. In *BSCL2* siRNA-transfected

HepG2 cells, *ATF4* and *GRP78* mRNA expression was increased by a little over 50% and *CHOP* by 100% (**Fig.8A**). PERK protein levels were also increased by 34% and 27% in *BSCL2*/*Bscl2* siRNA-transfected HepG2 cells as well as primary rat hepatocytes, respectively (**Fig.8B**). Our study revealed that Seipin deficiency induces expression of several markers of ER stress.

Discussion

In this study, we first confirmed that *Bscl2* is expressed in mouse liver (**Fig.1A**) albeit at a low protein level relative to testis, as previously reported for mRNA [65]. One group was recently able to detect the Seipin protein in human liver using LC/MS (humanproteomemap.org; [66]). We used siRNA to lower Seipin protein levels in hepatocytes (**Fig.1C**). This induced an increase in the number and the size of LD (**Fig.2A**). We also observed LD aggregation defects (**Fig.2B**), implying that Seipin plays a role in the generation, expansion and morphology of LD. These observed changes in shape and number of LD are similar to reported results in yeast, where a depletion of the *BSCL2* yeast ortholog *SEI1/FLD1* led to LD with irregular shapes and sizes [19, 21, 22, 24]. Up to 30% of the *SEI1/FLD1* deletion mutants contained one or a few supersized LD and about 60% of them contained an amorphous aggregation of LD [19].

Seipin has been suggested to act as a scaffold protein [30], however its function remains unclear. Seipin and SCD1 proteins are both localized in the ER [67, 68], and colocalize significantly in HepG2 cells (**Fig.6A**). Moreover, Seipin and SCD1 have opposite effects on LD homeostasis (**Fig.6C**). Taken together, our results suggest that Seipin and SCD1 are part of an ER-resident protein complex that controls LD formation. Different models for LD biogenesis consistently suggest that LD emerge from the ER [69]. The most accepted model posits that the accumulation of TAG between the bilayer leaflets of the ER membrane drives the genesis of nascent LD [28, 29]. In accordance with this, LD have been localized in close proximity to or even tethered to the ER in yeast [70, 71].

Seipin deficiency in hepatocytes caused lipid accumulation and was associated with increased expression of *CHOP*, *GRP78*, *ATF4* and the protein PERK (**Fig.8**), four markers of the unfolded protein response (UPR) to ER stress. A similar consequence of Seipin deficiency was previously observed in neuronal cells [72, 73]. In these prior studies, loss-of-function mutations in the Seipin protein induced a “seipinopathy”, a motor neuron disease associated with high LD formation and TAG storage as well as ER stress [74]. Interestingly, an activation of the UPR (PERK-eIF2α-ATF4) pathway, like the one seen in our *in vitro* models (**Fig.8**), can activate the expression of several

lipogenic genes (*Acc*/*ACC, Fas*/*FAS, Scd1*/*SCD1*) and the associated transcription factor SREBP-1c [11, 33, 35-37], thereby accentuating hepatic lipid synthesis/storage and potentially aggravating a nascent hepatic steatosis [33, 35, 37, 38].

The presence of smaller than normal LD in *C.elegans fat-6;fat-7* double mutants lacking most desaturases [75] suggests SCD activity is required for LD expansion. The MUFA/SFA intracellular lipid ratio also seems to play an important role in LD homeostasis, most notably on fusion and growth [76]. This is consistent with a role for SCD1, an enzyme that converts SFA into MUFA, in LD biogenesis and, by extension, TAG storage. For example, an increase in LD size within 3T3-L1 preadipocyte cells is associated with an increase in SCD1 expression and MUFA/SFA ratio [76]. The increase in SCD1 expression (**Fig.5B**) following our *BSCL2* knockdown was concomitant with an increase in the MUFA/SFA ratio (hence SCD1 activity; **Fig.6F**) and TAG synthesis (**Figs.5A and 7E**).

Moreover, high *Scd1* expression activates *de novo* lipogenesis via an elevation in hepatic SREBP-1c levels [77] that consequently increases the expression of lipogenic genes, including *Scd1* itself. The potential therefore exists for a reinforcing feedback loop to be established, leading to *Scd1* overexpression and enhancing hepatic lipogenesis following Seipin deficiency (**Fig.5**). Underlying the important role of SCD1 in TAG metabolism, DGAT (key enzymes implicated in TAG synthesis) colocalize with SCD1 in the ER [78] and could have synergistic interactions with Seipin [26]. The increase in number and size of LD we observed following *BSCL2* knockdown (**Figs.2A&6C**) could be due to lipid metabolism changes secondary to an increase in SCD1 activity. In agreement with this hypothesis, 3T3-L1 preadipocyte cells bearing a *Bscl2* mutation, and presumably possessing increased SCD1 activity, exhibit enhanced TAG synthesis [25]. Overall, increased SCD1 activity appears sufficient to explain most of the observed effects on fatty acid metabolism following *Bscl2*/*BSCL2* knockdown, including elevated PPARγ expression and CD36-mediated fatty acid uptake (**Fig.4**). In accordance with this, a *SCD1* knockdown reversed the effect of Seipin deficiency on LD formation (**Fig.6C**) and on lipid metabolism (**Fig.6D,E**) in hepatocytes. Inhibition of SCD1 activity is known to decrease PPARγ expression [79]. As CD36, the key cell surface receptor that facilitates

hepatic fatty acid uptake, is a direct transcriptional target of PPARγ [58], it is not surprising that SCD1 deficiency alone decreases oleate uptake (**Fig.6D**).

Recent studies have shown that the adipose tissue plays a major role in the establishment of hepatic steatosis in *Bscl2*$^{-/-}$ mice [7, 9, 15]. Expressing Seipin in adipose tissue alone is sufficient to rescue lipodystrophy, hepatic steatosis and insulin resistance in *Bscl2*$^{-/-}$ mice [15]. Chen and collaborators also reported that mice with a specific hepatic deletion of Seipin (*Bscl2*$^{Li-/-}$) did not show increased lipid deposition in the liver on a standard chow diet [80]. Such striking results led these researchers to conclude that Seipin does not play a role in hepatic steatosis. However, our study clearly shows an effect of Seipin deficiency on fat accumulation in hepatocytes. The discrepancy between these *in vivo* results and our observations is probably due to the storage of circulating lipids, in the form of free or esterified fatty acids in the blood, within the adipose tissue. In *Bscl2*$^{-/-}$ mice, the absence of adipose tissue causes an accumulation of plasma fatty acids and a compensatory fatty acid uptake (leading to steatosis) in the liver. Consequently, *Bscl2*$^{-/-}$ mice do not suffer from hypertriglyceridemia [7, 8]. *Bscl2*$^{Li-/-}$ mice possess a normal adipose tissue that stores excess fat originating from a standard chow diet. However, a high fat diet leads to a strong increase in circulating lipid levels, and under these conditions both *Bscl2*$^{Li+/+}$ and *Bscl2*$^{Li-/-}$ mice develop hepatic steatosis [80]. Presumably, the storage capacity of both the adipose tissue and the liver becomes saturated in these mice, precluding the observation of more subtle intracellular differences. Consistent with a cell autonomous role for Seipin in hepatic fat accumulation, we show that the expression of several genes implicated in LD homeostasis is elevated in the liver of *Bscl2*$^{-/-}$ mice (*Plin5* and *Cidea*; **Fig.3**). Seipin does not appear to be necessary for the formation of a LD, notably in *Bscl2/BLSC2*$^{-/-}$ hepatocytes, but this does not exclude a role in lipid storage. In support of such a role, Yang *et al.* have suggested that Seipin restricts lipogenesis and LD accumulation in non-adipocyte cells [27]. The authors show that Seipin overexpression inhibits ectopic lipid-induced LD formation in a mouse hepatocyte cell line (AML-12 cells) and distinguish two functions for the Seipin protein, one in adipocyte maturation (via its C-terminal domain) and another in the control of intracellular lipid levels (via a conserved core sequence) in non-adipocyte cells [27]. Therefore, we argue that the endogenously expressed Seipin protein plays a role in LD

homeostasis and TAG storage in hepatocytes.

Several previous studies have clearly demonstrated that Seipin deficiency in both mice and humans leads to insulin resistance [7-9]. Surprisingly, we observed that Seipin deficiency increased basal phosphorylation of AKT, ERK and P70S6K proteins, suggesting an increase in insulin sensitivity (**Fig.7A**). In agreement with this interpretation, Chen and collaborators observed improved hepatic insulin signaling in *Bscl2*$^{-/-}$ mice, as measured by insulin clamp [16]. To explain their result, the authors suggest that the enhanced insulin sensitivity observed after 16h fasting stems from increased levels of insulin receptors and downstream signaling effectors such as IRS1 and AKT [16]. The increased basal phosphorylation of insulin signaling pathway proteins observed in our *BSCL2* siRNA-transfected hepatocytes may be explained, at least in part, by the effect of Seipin deficiency on SCD1 activity (**Fig.6F**), as an increase in MUFA has been shown to stimulate insulin signaling [81-85].

Insulin negatively regulates the expression of gluconeogenic genes *Pepck* and *G6pc*, and increases expression of *Gck*, the enzyme responsible for the first step of hepatic glycolysis [86]. The modulation of glucose metabolism markers observed in our study (**Fig.7C**) is somewhat consistent with an activation of the insulin signaling proteins following Seipin deficiency, with the notable exception of *Pepck* gene expression being specifically elevated in fasted mice. This paradox might be explained by the activation of ER stress in Seipin deficient hepatocytes (**Fig.8**). PEPCK expression is activated by ER stress through promoter binding by the ATF4 transcription factor, leading to increased transcription [87]. Additionally, *Pepck* expression could enhance gluconeogenesis in Seipin deficient cells, leading to increased intracellular glucose concentration and the reduction of AMPK phosphorylation we observe (**Fig.7B**) [88, 89]. Interestingly, decreased AMPK phosphorylation/activity can also lead to an activation of its targets proteins, notably the lipogenic enzyme ACC [90]. Therefore, a combined increase in gluconeogenesis and insulin signaling can lead to further activation of lipogenic markers such as FAS, SCD1 and ACC (**Fig.5**) [91-97].

We showed that Seipin depletion in cultured hepatocytes leads to an increase in LD number and size. These changes in LD homeostasis are probably due to an upregulation

of lipid metabolism, characterized by an increase in SCD1 activity leading to a higher MUFA/SFA ratio. In accordance with this, a *SCD1* knockdown reversed the LD formation defects and the changes in lipid metabolism homeostasis associated with Seipin depletion. Interestingly, Seipin and SCD1 also colocalize, leading us to propose a functional interaction within the ER membrane whereby Seipin controls lipid metabolism and storage through SCD1 activity and LD formation.

Acknowledgements

We wish to thank Dr. Jocelyne Magre (University of Nantes, France) for kindly providing us with mRNA and protein extracts from *Bscl2*$^{-/-}$ mice, as well as Dr. Xiaoqin Ye (University of Georgia, USA) for samples of *Bscl2*$^{-/-}$ mouse liver. We also thank Denis Flipo for his precious help with confocal microscopy, the laboratory of Dr. Diana Averill for primary rat hepatocytes and Dr. Daniel Boismenu for his help with data analysis and discussion.

The Discovery Grants Program of the National Science and Engineering Research Council of Canada (NSERC) funded this research. MAL and SL were supported by the Fond de Recherche du Québec-Nature et Technologie (FRQNT) fellowships.

Conflict of Interest

The authors declare that they have no competing interests.

References

1. Garg, A., *Clinical review#: Lipodystrophies: genetic and acquired body fat disorders.* J Clin Endocrinol Metab, 2011. **96**(11): p. 3313-25.
2. Berardinelli, W., *An undiagnosed endocrinometabolic syndrome: report of 2 cases.* J Clin Endocrinol Metab, 1954. **14**(2): p. 193-204.
3. Seip, M., *Lipodystrophy and gigantism with associated endocrine manifestations. A new diencephalic syndrome?* Acta Paediatr, 1959. **48**: p. 555-74.
4. Agarwal, A.K. and A. Garg, *Seipin: a mysterious protein.* Trends Mol Med, 2004. **10**(9): p. 440-4.
5. Magre, J., et al., *Identification of the gene altered in Berardinelli-Seip congenital lipodystrophy on chromosome 11q13.* Nat Genet, 2001. **28**(4): p. 365-70.
6. Agarwal, A.K. and A. Garg, *Congenital generalized lipodystrophy: significance of triglyceride biosynthetic pathways.* Trends Endocrinol Metab, 2003. **14**(5): p. 214-21.
7. Cui, X., et al., *Seipin ablation in mice results in severe generalized lipodystrophy.* Hum Mol Genet, 2011. **20**(15): p. 3022-30.
8. Prieur, X., et al., *Thiazolidinediones partially reverse the metabolic disturbances observed in Bscl2/seipin-deficient mice.* Diabetologia, 2013. **56**(8): p. 1813-25.
9. Chen, W., et al., *Berardinelli-seip congenital lipodystrophy 2/seipin is a cell-autonomous regulator of lipolysis essential for adipocyte differentiation.* Mol Cell Biol, 2012. **32**(6): p. 1099-111.
10. Payne, V.A., et al., *The human lipodystrophy gene BSCL2/seipin may be essential for normal adipocyte differentiation.* Diabetes, 2008. **57**(8): p. 2055-60.
11. Liu, L., et al., *Adipose-specific knockout of SEIPIN/BSCL2 results in progressive lipodystrophy.* Diabetes, 2014. **63**(7): p. 2320-31.
12. Unger, R.H., *Lipotoxic diseases.* Annu Rev Med, 2002. **53**: p. 319-36.
13. van Herpen, N.A. and V.B. Schrauwen-Hinderling, *Lipid accumulation in non-adipose tissue and lipotoxicity.* Physiol Behav, 2008. **94**(2): p. 231-41.
14. Szendroedi, J. and M. Roden, *Ectopic lipids and organ function.* Curr Opin Lipidol, 2009. **20**(1): p. 50-6.
15. Gao, M., et al., *Expression of seipin in adipose tissue rescues lipodystrophy, hepatic steatosis and insulin resistance in seipin null mice.* Biochem Biophys Res Commun, 2015. **460**(2): p. 143-50.
16. Chen, W., et al., *Molecular mechanisms underlying fasting modulated liver insulin sensitivity and metabolism in male lipodystrophic Bscl2/Seipin-deficient mice.* Endocrinology, 2014. **155**(11): p. 4215-25.
17. Cartwright, B.R. and J.M. Goodman, *Seipin: from human disease to molecular mechanism.* J Lipid Res, 2012. **53**(6): p. 1042-55.
18. Fei, W., X. Du, and H. Yang, *Seipin, adipogenesis and lipid droplets.* Trends Endocrinol Metab, 2011. **22**(6): p. 204-10.
19. Fei, W., et al., *Fld1p, a functional homologue of human seipin, regulates the size of lipid droplets in yeast.* J Cell Biol, 2008. **180**(3): p. 473-82.
20. Wolinski, H., et al., *A role for seipin in lipid droplet dynamics and inheritance in yeast.* J Cell Sci, 2011. **124**(Pt 22): p. 3894-904.

21. Wolinski, H., et al., *Seipin is involved in the regulation of phosphatidic acid metabolism at a subdomain of the nuclear envelope in yeast.* Biochim Biophys Acta, 2015. **1851**(11): p. 1450-64.
22. Wang, C.W., Y.H. Miao, and Y.S. Chang, *Control of lipid droplet size in budding yeast requires the collaboration between Fld1 and Ldb16.* J Cell Sci, 2014. **127**(Pt 6): p. 1214-28.
23. Fei, W., et al., *A role for phosphatidic acid in the formation of "supersized" lipid droplets.* PLoS Genet, 2011. **7**(7): p. e1002201.
24. Szymanski, K.M., et al., *The lipodystrophy protein seipin is found at endoplasmic reticulum lipid droplet junctions and is important for droplet morphology.* Proc Natl Acad Sci U S A, 2007. **104**(52): p. 20890-5.
25. Fei, W., et al., *Molecular characterization of seipin and its mutants: implications for seipin in triacylglycerol synthesis.* J Lipid Res, 2011. **52**(12): p. 2136-47.
26. Tian, Y., et al., *Tissue-autonomous function of Drosophila seipin in preventing ectopic lipid droplet formation.* PLoS Genet, 2011. **7**(4): p. e1001364.
27. Yang, W., et al., *Seipin differentially regulates lipogenesis and adipogenesis through a conserved core sequence and an evolutionarily acquired C-terminus.* Biochem J, 2013. **452**(1): p. 37-44.
28. Harris, C.A., et al., *DGAT enzymes are required for triacylglycerol synthesis and lipid droplets in adipocytes.* J Lipid Res, 2011. **52**(4): p. 657-67.
29. Brasaemle, D.L. and N.E. Wolins, *Packaging of fat: an evolving model of lipid droplet assembly and expansion.* J Biol Chem, 2012. **287**(4): p. 2273-9.
30. Talukder, M.M., et al., *Seipin oligomers can interact directly with AGPAT2 and lipin 1, physically scaffolding critical regulators of adipogenesis.* Mol Metab, 2015. **4**(3): p. 199-209.
31. Yang, W., et al., *BSCL2/seipin regulates adipogenesis through actin cytoskeleton remodelling.* Hum Mol Genet, 2014. **23**(2): p. 502-13.
32. Bi, J., et al., *Seipin promotes adipose tissue fat storage through the ER Ca(2)(+)-ATPase SERCA.* Cell Metab, 2014. **19**(5): p. 861-71.
33. Puri, P., et al., *Activation and dysregulation of the unfolded protein response in nonalcoholic fatty liver disease.* Gastroenterology, 2008. **134**(2): p. 568-76.
34. Puri, V., et al., *Fat-specific protein 27, a novel lipid droplet protein that enhances triglyceride storage.* J Biol Chem, 2007. **282**(47): p. 34213-8.
35. Fang, D.L., et al., *Endoplasmic reticulum stress leads to lipid accumulation through upregulation of SREBP-1c in normal hepatic and hepatoma cells.* Mol Cell Biochem, 2013. **381**(1-2): p. 127-37.
36. Rinella, M.E., et al., *Dysregulation of the unfolded protein response in db/db mice with diet-induced steatohepatitis.* Hepatology, 2011. **54**(5): p. 1600-9.
37. Gentile, C.L., M. Frye, and M.J. Pagliassotti, *Endoplasmic reticulum stress and the unfolded protein response in nonalcoholic fatty liver disease.* Antioxid Redox Signal, 2011. **15**(2): p. 505-21.
38. Zhang, X.Q., et al., *Role of endoplasmic reticulum stress in the pathogenesis of nonalcoholic fatty liver disease.* World J Gastroenterol, 2014. **20**(7): p. 1768-76.
39. Zhang, K., et al., *The unfolded protein response transducer IRE1alpha prevents ER stress-induced hepatic steatosis.* EMBO J, 2011. **30**(7): p. 1357-75.

40. Zhang, C., et al., *Endoplasmic reticulum-tethered transcription factor cAMP responsive element-binding protein, hepatocyte specific, regulates hepatic lipogenesis, fatty acid oxidation, and lipolysis upon metabolic stress in mice.* Hepatology, 2012. **55**(4): p. 1070-82.
41. Rutkowski, D.T. and R.J. Kaufman, *A trip to the ER: coping with stress.* Trends Cell Biol, 2004. **14**(1): p. 20-8.
42. Harbrecht, B.G., et al., *cAMP inhibits inducible nitric oxide synthase expression and NF-kappaB-binding activity in cultured rat hepatocytes.* J Surg Res, 2001. **99**(2): p. 258-64.
43. Harbrecht, B.G., et al., *Glucagon inhibits hepatocyte nitric oxide synthesis.* Arch Surg, 1996. **131**(12): p. 1266-72.
44. Bligh, E.G. and W.J. Dyer, *A rapid method of total lipid extraction and purification.* Can J Biochem Physiol, 1959. **37**(8): p. 911-7.
45. Ralston, J.C., et al., *Inhibition of stearoyl-CoA desaturase-1 in differentiating 3T3-L1 preadipocytes upregulates elongase 6 and downregulates genes affecting triacylglycerol synthesis.* Int J Obes (Lond), 2014. **38**(11): p. 1449-56.
46. Fernandez, C., et al., *Altered desaturation and elongation of fatty acids in hormone-sensitive lipase null mice.* PLoS One, 2011. **6**(6): p. e21603.
47. Attie, A.D., et al., *Relationship between stearoyl-CoA desaturase activity and plasma triglycerides in human and mouse hypertriglyceridemia.* J Lipid Res, 2002. **43**(11): p. 1899-907.
48. Stremmel, W. and P.D. Berk, *Hepatocellular influx of [14C]oleate reflects membrane transport rather than intracellular metabolism or binding.* Proc Natl Acad Sci U S A, 1986. **83**(10): p. 3086-90.
49. Pohl, J., A. Ring, and W. Stremmel, *Uptake of long-chain fatty acids in HepG2 cells involves caveolae: analysis of a novel pathway.* J Lipid Res, 2002. **43**(9): p. 1390-9.
50. Bolker, H.I., et al., *The incorporation of acetate-1-C14 into cholesterol and fatty acids by surviving tissues of normal and scorbutic guinea pigs.* J Exp Med, 1956. **103**(2): p. 199-205.
51. Jin, F.Y., V.S. Kamanna, and M.L. Kashyap, *Niacin accelerates intracellular ApoB degradation by inhibiting triacylglycerol synthesis in human hepatoblastoma (HepG2) cells.* Arterioscler Thromb Vasc Biol, 1999. **19**(4): p. 1051-9.
52. Jiang, M., et al., *Lack of testicular seipin causes teratozoospermia syndrome in men.* Proc Natl Acad Sci U S A, 2014. **111**(19): p. 7054-9.
53. Wu, L., et al., *Cidea controls lipid droplet fusion and lipid storage in brown and white adipose tissue.* Sci China Life Sci, 2014. **57**(1): p. 107-16.
54. Wang, H., et al., *Perilipin 5, a lipid droplet-associated protein, provides physical and metabolic linkage to mitochondria.* J Lipid Res, 2011. **52**(12): p. 2159-68.
55. Beller, M., et al., *COPI complex is a regulator of lipid homeostasis.* PLoS Biol, 2008. **6**(11): p. e292.
56. Guo, Y., et al., *Functional genomic screen reveals genes involved in lipid-droplet formation and utilization.* Nature, 2008. **453**(7195): p. 657-61.
57. Soni, K.G., et al., *Coatomer-dependent protein delivery to lipid droplets.* J Cell Sci, 2009. **122**(Pt 11): p. 1834-41.

58. He, J., et al., *The emerging roles of fatty acid translocase/CD36 and the aryl hydrocarbon receptor in fatty liver disease.* Exp Biol Med (Maywood), 2011. **236**(10): p. 1116-21.
59. Cheon, Y., et al., *Induction of overlapping genes by fasting and a peroxisome proliferator in pigs: evidence of functional PPARalpha in nonproliferating species.* Am J Physiol Regul Integr Comp Physiol, 2005. **288**(6): p. R1525-35.
60. Louet, J.F., et al., *Long-chain fatty acids regulate liver carnitine palmitoyltransferase I gene (L-CPT I) expression through a peroxisome-proliferator-activated receptor alpha (PPARalpha)-independent pathway.* Biochem J, 2001. **354**(Pt 1): p. 189-97.
61. Berardinelli, S.D., R.M. Fischer, and I. Katz, *Congenital absence of the pectoral muscle.* Am J Roentgenol Radium Ther Nucl Med, 1956. **76**(3): p. 599-604.
62. Thomas, S.E., et al., *Diabetes as a disease of endoplasmic reticulum stress.* Diabetes Metab Res Rev, 2010. **26**(8): p. 611-21.
63. Kaufman, R.J., *Orchestrating the unfolded protein response in health and disease.* J Clin Invest, 2002. **110**(10): p. 1389-98.
64. Lee, J.S., et al., *Pharmacologic ER stress induces non-alcoholic steatohepatitis in an animal model.* Toxicol Lett, 2012. **211**(1): p. 29-38.
65. Chen, W., et al., *The human lipodystrophy gene product Berardinelli-Seip congenital lipodystrophy 2/seipin plays a key role in adipocyte differentiation.* Endocrinology, 2009. **150**(10): p. 4552-61.
66. Kim, M.S., et al., *A draft map of the human proteome.* Nature, 2014. **509**(7502): p. 575-81.
67. Lundin, C., et al., *Membrane topology of the human seipin protein.* FEBS Lett, 2006. **580**(9): p. 2281-4.
68. Ntambi, J.M., et al., *Loss of stearoyl-CoA desaturase-1 function protects mice against adiposity.* Proc Natl Acad Sci U S A, 2002. **99**(17): p. 11482-6.
69. Walther, T.C. and R.V. Farese, Jr., *The life of lipid droplets.* Biochim Biophys Acta, 2009. **1791**(6): p. 459-66.
70. Novikoff, A.B., et al., *Organelle relationships in cultured 3T3-L1 preadipocytes.* J Cell Biol, 1980. **87**(1): p. 180-96.
71. Perktold, A., et al., *Organelle association visualized by three-dimensional ultrastructural imaging of the yeast cell.* FEMS Yeast Res, 2007. **7**(4): p. 629-38.
72. Ito, D. and N. Suzuki, *Seipinopathy: a novel endoplasmic reticulum stress-associated disease.* Brain, 2009. **132**(Pt 1): p. 8-15.
73. Yagi, T., et al., *N88S seipin mutant transgenic mice develop features of seipinopathy/BSCL2-related motor neuron disease via endoplasmic reticulum stress.* Hum Mol Genet, 2011. **20**(19): p. 3831-40.
74. Holtta-Vuori, M., et al., *Alleviation of seipinopathy-related ER stress by triglyceride storage.* Hum Mol Genet, 2013. **22**(6): p. 1157-66.
75. Shi, X., et al., *Regulation of lipid droplet size and phospholipid composition by stearoyl-CoA desaturase.* J Lipid Res, 2013. **54**(9): p. 2504-14.
76. Arisawa, K., et al., *Changes in the phospholipid fatty acid composition of the lipid droplet during the differentiation of 3T3-L1 adipocytes.* J Biochem, 2013. **154**(3): p. 281-9.

77. Miyazaki, M., et al., *Hepatic stearoyl-CoA desaturase-1 deficiency protects mice from carbohydrate-induced adiposity and hepatic steatosis.* Cell Metab, 2007. **6**(6): p. 484-96.
78. Man, W.C., et al., *Colocalization of SCD1 and DGAT2: implying preference for endogenous monounsaturated fatty acids in triglyceride synthesis.* J Lipid Res, 2006. **47**(9): p. 1928-39.
79. Kim, E., et al., *Inhibition of stearoyl-CoA desaturase1 activates AMPK and exhibits beneficial lipid metabolic effects in vitro.* Eur J Pharmacol, 2011. **672**(1-3): p. 38-44.
80. Chen, W., et al., *Molecular mechanisms underlying fasting modulated liver insulin sensitivity and metabolism in male lipodystrophic Bscl2/Seipin-deficient mice.* Endocrinology, 2014: p. en20141292.
81. Coll, T., et al., *Oleate reverses palmitate-induced insulin resistance and inflammation in skeletal muscle cells.* J Biol Chem, 2008. **283**(17): p. 11107-16.
82. Nardi, F., et al., *Enhanced insulin sensitivity associated with provision of mono and polyunsaturated fatty acids in skeletal muscle cells involves counter modulation of PP2A.* PLoS One, 2014. **9**(3): p. e92255.
83. Xiao, C., et al., *Differential effects of monounsaturated, polyunsaturated and saturated fat ingestion on glucose-stimulated insulin secretion, sensitivity and clearance in overweight and obese, non-diabetic humans.* Diabetologia, 2006. **49**(6): p. 1371-9.
84. Vessby, B., et al., *Substituting dietary saturated for monounsaturated fat impairs insulin sensitivity in healthy men and women: The KANWU Study.* Diabetologia, 2001. **44**(3): p. 312-9.
85. Salvado, L., et al., *Oleate prevents saturated-fatty-acid-induced ER stress, inflammation and insulin resistance in skeletal muscle cells through an AMPK-dependent mechanism.* Diabetologia, 2013. **56**(6): p. 1372-82.
86. O'Brien, R.M. and D.K. Granner, *Regulation of gene expression by insulin.* Physiol Rev, 1996. **76**(4): p. 1109-61.
87. Mendez-Lucas, A., et al., *Mitochondrial phosphoenolpyruvate carboxykinase (PEPCK-M) is a pro-survival, endoplasmic reticulum (ER) stress response gene involved in tumor cell adaptation to nutrient availability.* J Biol Chem, 2014. **289**(32): p. 22090-102.
88. Foufelle, F. and P. Ferre, *New perspectives in the regulation of hepatic glycolytic and lipogenic genes by insulin and glucose: a role for the transcription factor sterol regulatory element binding protein-1c.* Biochem J, 2002. **366**(Pt 2): p. 377-91.
89. Foretz, M., et al., *AMP-activated protein kinase inhibits the glucose-activated expression of fatty acid synthase gene in rat hepatocytes.* J Biol Chem, 1998. **273**(24): p. 14767-71.
90. Zhou, G., et al., *Role of AMP-activated protein kinase in mechanism of metformin action.* J Clin Invest, 2001. **108**(8): p. 1167-74.
91. Decaux, J.F., B. Antoine, and A. Kahn, *Regulation of the expression of the L-type pyruvate kinase gene in adult rat hepatocytes in primary culture.* J Biol Chem, 1989. **264**(20): p. 11584-90.

92. Prip-Buus, C., et al., *Induction of fatty-acid-synthase gene expression by glucose in primary culture of rat hepatocytes. Dependency upon glucokinase activity.* Eur J Biochem, 1995. **230**(1): p. 309-15.
93. O'Callaghan, B.L., et al., *Glucose regulation of the acetyl-CoA carboxylase promoter PI in rat hepatocytes.* J Biol Chem, 2001. **276**(19): p. 16033-9.
94. Koo, S.H., A.K. Dutcher, and H.C. Towle, *Glucose and insulin function through two distinct transcription factors to stimulate expression of lipogenic enzyme genes in liver.* J Biol Chem, 2001. **276**(12): p. 9437-45.
95. Waters, K.M. and J.M. Ntambi, *Insulin and dietary fructose induce stearoyl-CoA desaturase 1 gene expression of diabetic mice.* J Biol Chem, 1994. **269**(44): p. 27773-7.
96. Foufelle, F., et al., *Glucose stimulation of lipogenic enzyme gene expression in cultured white adipose tissue. A role for glucose 6-phosphate.* J Biol Chem, 1992. **267**(29): p. 20543-6.
97. Jones, B.H., et al., *Glucose induces expression of stearoyl-CoA desaturase in 3T3-L1 adipocytes.* Biochem J, 1998. **335 (Pt 2)**: p. 405-8.

Table 1. List of antibodies used for immunoblotting

Antibody target	Manufacturer	Catalog number	Concentration used
ACC	Cell Signaling Tech.	3662	1: 1000
AGPAT2	Abcam	ab62599	1: 500
AKT	Cell Signaling Tech.	9272	1: 1000
AMPK α	Cell Signaling Tech.	2532	1: 1000
ATGL	Cayman Chemical	10006409	1: 1000
β-Actin	Cell Signaling Tech.	4970	1: 1000
BSCL2/Seipin	Santa Cruz Biotech.	sc-55987	1: 200
CD36	Abcam	ab78054	1: 1000
ERK1/2	Cell Signaling Tech.	9103	1: 1000
FAS	Santa Cruz Biotech.	sc-55580	1: 1000
GAPDH	Cell Signaling Tech.	5174	1: 1000
IRS1	Cell Signaling Tech.	2382	1: 1000
p-AKT (Thr 308)	Cell Signaling Tech.		1: 1000
p-AKT (Ser 473)	Cell Signaling Tech.	4060	1: 1000
p-AMPKα (Thr 172)	Cell Signaling Tech.	2535	1: 1000
p-ERK1/2 (Thr 202/Tyr 204)	Cell Signaling Tech.	4370	1: 1000
p-IRS1 (Tyr 612)	Santa Cruz Biotech.	sc-17195-R	1: 1000
p-P70S6K (Thr389)	Cell Signaling Tech.	9234	1: 1000
P70S6K	Cell Signaling Tech.	9202	1: 1000
PERK	Cell Signaling Tech.	3192	1: 1000
PPARα	Santa Cruz Biotech.	sc-9000	1: 1000
PPARγ	Cell Signaling Tech.	2435	1: 1000
SCD1	Abcam	ab19862	1: 1000
SREBP-1	Santa Cruz Biotech.	sc-366	1: 1000
α-Tubulin	Cell Signaling Tech.	2144	1: 1000
goat IgG (HRP-linked)	Santa Cruz Biotech.	sc-2020	1: 1000
mouse IgG (HRP-linked)	Cell Signaling Tech.	7076	1: 1000
rabbit IgG (HRP-linked)	Cell Signaling Tech.	7074	1: 1000

Figure Legends

Figure 1. Seipin expression in hepatocytes

(**A**) Seipin expression was evaluated by Western blot in protein extracts prepared from rat testis, rat adipose tissue (AT), primary rat hepatocytes and HepG2 cells (***left panels***), as well as liver of WT and *Bscl2*$^{-/-}$ mice (***right panels***). GAPDH or α-Tubulin were used as loading controls. Tissues from 3 different animals or from 3 different cell passages were tested (n=3). (**B**) Immunohistochemical staining for Seipin (brown color) in HepG2 cells was followed by nucleus counterstaining (blue). A negative control without primary antibody is presented for comparison. The images are representative of three different cell experiments (n=3). Bar: 100µm. (**C**) Seipin expression was evaluated by Western blot in HepG2 cells (***left panels***) and rat primary hepatocytes (***right panels***) transfected with a *Bscl2* siRNA (siBSCL2) or a negative control (CTRL). Protein levels evaluated by densitometry were normalized against GAPDH (loading control) and negative controls. Graphs combine results from 5 independent experiments (n=5). ** $p<0.002$. *** $p<0.001$.

Figure 2. Seipin deficiency affects LD formation, expansion and aggregation

(**A**) Rat primary hepatocytes and HepG2 cells were transfected with negative control (CTRL) or *Bscl2* siRNA (siBSCL2), and treated (or not) with 100µM oleate for 24h. Cells were stained with Bodipy 493/503 to allow quantification of LD number and size. Bars: 100 µm. Graphs combine results from 5 independent experiments (n=5). Results are presented for number and size of LD as number of LD per 100 cells and diameter of LD (µm), respectively. * $p<0.05$. ** $p<0.002$. *** $p<0.001$. (**B**) Time-lapse analysis of LD formation in control and Seipin-deficient HepG2 cells. Cells were transfected with negative control (CTRL) or *BSCL2* siRNA (siBSCL2), incubated with 100µM oleate and Bodipy 493/502 and imaged by confocal microscopy in a 37°C chamber supplied with 5% CO_2. Images were taken every 10min over a period of 16.5h. T=0 in figures corresponds to hour 14 of the time-lapse. Outlined in blue: LD expansion/persistence,

red: LD aggregation, yellow: LD degradation. Images are representative of five different experiments (n=5). Bar: 35µm.

Figure 3. Seipin deficiency modulates expression of LD biogenesis genes

Expression of genes involved in LD formation and stability, as well as lipolysis, was evaluated by qRT-PCR in HepG2 cells transfected overnight with negative control (CTRL) or *BSCL2* siRNA (siBSCL2), and in the liver of wildtype (WT) and *Bscl2*$^{-/-}$ (KO) mice fasted for 24h or fed *ad libitum*. Results were normalized against *HPRT1* or *Cyclophilin A* (CYCLO) and negative controls where appropriate. Graphs combine results from 5 independent experiments (HepG2 cells) or 5 different liver extracts obtained from *Bscl2*$^{-/-}$ mice (n=5). * $p<0.05$. ** $p<0.002$. *** $p<0.001$. **** $p<0.0001$. NS: not significant.

Figure 4. Seipin deficiency increases fatty acid uptake in hepatocytes

(**A**) HepG2 cells and rat primary hepatocytes were transfected with negative control (CTRL) or *BSCL2* siRNA (siBSCL2) and incubated with [^{3}H]oleate for 10min. Incorporated radioactivity was measured in cell lysates, normalized against negative controls and presented as CPM/mg of total protein. Graphs combine results from 5 independent experiments (n=5). (**B**) HepG2 cells were transfected with negative control (CTRL) or *BSCL2* siRNA (siBSCL2), and Western blot analyses were performed to measure the expression of proteins involved in fatty acid uptake (PPARγ and CD36). The expression level of AGPAT2, implicated in the PPARγ signaling pathway, is also presented. Protein levels evaluated by densitometry were normalized against GAPDH (loading control) and negative controls. Graphs combine results from 5 independent experiments (n=5). * $p<0.05$. ** $p<0.002$. *** $p<0.001$.

Figure 5. Seipin deficiency increases *de novo* lipogenesis in hepatocytes

(**A**) HepG2 cells were transfected with negative control (CTRL) or *BSCL2* siRNA (siBSCL2) and incubated with [^{14}C]acetate for 4h. Incorporated radioactivity was

measured in extracted total lipids, triglycerides and diacylglycerol, and presented as CPM/mg of total protein. Graphs combine results from 5 independent experiments (n=5). (**B**) Expression of proteins involved in lipid metabolism (ACC, FAS, mature SREBP-1c, SCD1, ATGL and PPARα) was measured by Western blot in HepG2 cells transfected with negative control (CTRL) or *BSCL2* siRNA (siBSCL2). Protein levels evaluated by densitometry were normalized against GAPDH and negative controls. Graphs combine results from 5 independent experiments (n=5). (**C**) Expression of mature SREBP-1c was also measured in liver extracts from wildtype (WT) and *Bscl2*$^{-/-}$ (KO) mice fasted for 24h or fed *ad libitum*. Protein levels evaluated by densitometry were normalized against β-Actin. Graph combines results from 5 different liver extracts (n=5). * $p<0.05$. ** $p<0.002$. *** $p<0.001$.

Figure 6. SCD1 knockdown reverses the phenotype observed in Seipin-deficient hepatocytes

(**A**) Confocal images of HepG2 cells showing staining for Seipin/BSCL2 (red), SCD1 (green) and cell nuclei (DAPI; blue). Merged (and zoom) image shows sites of colocalization (yellow). Images are representative of five different experiments (n=5). Bar: 35μm. (**B**) SCD1 expression in protein extracts prepared from HepG2 cells transfected with a *SCD1* siRNA (siSCD1) or a negative control (CTRL) were evaluated by Western blot. Protein levels evaluated by densitometry were normalized against GAPDH and negative control. Graph combines results from 5 independent experiments (n=5). (**C**) HepG2 cells were transfected with negative control (CTRL), *SCD1*, *BSCL2*, or cotransfected with both *SCD1* and *BSCL2* siRNA. Cells were then treated (or not) with 100μM oleate for 24h. Cells were stained with Bodipy 493/503 to allow quantification of LD number and size. Bar: 100μm. Graphs combine results from 5 independent experiments (n=5). Results are presented for number and size of LD as number of LD per 100 cells and diameter of LD (μm), respectively. (**D**) HepG2 cells were transfected with negative control (CTRL), *SCD1*, *BSCL2*, or with both *SCD1* and *BSCL2* siRNA. Cells were incubated with [^{3}H]oleate for 10min. Incorporated radioactivity was measured in cell lysates, normalized against negative controls and presented as CPM/mg of total

protein. Graphs combine results from 5 independent experiments (n=5). (**E**) HepG2 cells were transfected with negative control (CTRL), *SCD1*, *BSCL2*, or with both *SCD1* and *BSCL2* siRNA(s). Cells were incubated with [^{14}C]acetate for 4h. Incorporated radioactivity was measured in extracted total lipids, triglycerides and diacylglycerol, and presented as CPM/mg of total protein. Graphs combine results from 5 independent experiments (n=5). (**F**) The total SFA (16:0 and 18:0) and MUFA (16:1n7 and 18:1n9) cellular content of HepG2 cells transfected with negative control (CTRL), *SCD1*, *BSCL2* or cotransfected with both *SCD1* and *BSCL2* siRNA was determined by gas chromatography. The results of 5 independent experiments (n=5) are presented as mean ± SEM and compared to CTRL for statistical analyses. * $p<0.05$. ** $p<0.002$. *** $p<0.001$.

Figure 7. Seipin deficiency increases basal phosphorylation of insulin-signaling proteins

(**A**) HepG2 cells were transfected with negative control (CTRL) or *BSCL2* siRNA (siBSCL2) and incubated with 100nM insulin for 10min. AKT, ERK, mTOR and P70S6K protein expression as well as their phosphorylation states were evaluated by Western blot densitometry. Phosphorylated protein levels were normalized against total protein levels. Graphs combine results from 5 independent experiments (n=5). (**B**) AKT, IRS1 and AMPK protein expression levels and phosphorylation states were evaluated by Western blot densitometry in liver extracts from wildtype (WT) and *Bscl2*$^{-/-}$ (KO) mice fasted for 24h or fed *ad libitum*. Phosphorylated protein levels were normalized against total protein levels. Graphs combine results from 5 different liver extracts (n=5). (**C**) Expression of genes involved in glucose metabolism (*Pepck*, *Gck* and *G6pc*) was measured by qRT-PCR in the liver of wildtype (WT) and *Bscl2*$^{-/-}$ (KO) mice fasted for 24h or fed *ad libitum*. Results were normalized to *Cyclophilin A* (CYCLO). Graphs combine results from 5 different liver extracts (n=5). KO results were compared to WT for statistical analyses. (**D)** HepG2 cells were transfected with negative control (CTRL) or *BSCL2* siRNA (siBSCL2). Cells were then incubated with [^{3}H]oleate for 10min in the presence or absence of 100nM insulin. Incorporated radioactivity was measured in cell lysates, normalized against non-stimulated negative control and presented as CPM/mg of

total protein. Graph combines results from 5 independent experiments (n=5). (**E**) HepG2 cells were transfected with negative control (CTRL) or *BSCL2* siRNA (siBSCL2) and incubated with [^{14}C]acetate for 4h in the presence or absence of 100nM insulin for the last 10min. Incorporated radioactivity was measured in extracted total lipids, triglycerides and diacylglycerol, and presented as CPM/mg of total protein. Graphs combine results from 5 independent experiments (n=5). * $p<0.05$. ** $p<0.002$. *** $p<0.001$. **** $p<0.0001$. NS: not significant.

Figure 8. Seipin deficiency increases the expression of ER stress markers

(**A**) Expression of genes involved in ER stress (*ATF4, GRP78 and CHOP*) was measured by qRT-PCR in HepG2 cells transfected with negative control (CTRL) or *BSCL2* siRNA (siBSCL2). Results were normalized against *HPRT1* and negative controls. Graphs combine results from 5 independent experiments (n=5). (**B**) PERK expression was measured by Western blot in HepG2 cells and primary rat hepatocytes transfected with negative control (CTRL) or *BSCL2/Bscl2* siRNA (siBSCL2). Protein levels evaluated by densitometry were normalized against α-Tubulin and negative controls**.** Graphs combine results from 5 independent experiments (n=5). * $p<0.05$. ** $p<0.002$.

A

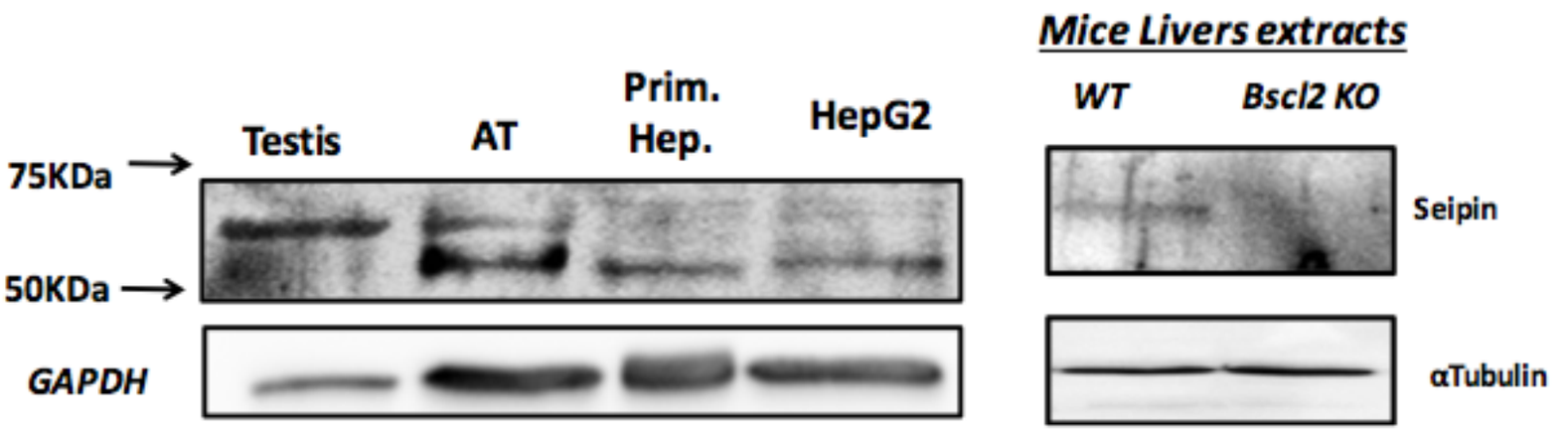
Mice Livers extracts
WT
Bscl2 KO
Testis
AT
Prim. Hep.
HepG2
75KDa
50KDa
GAPDH
Seipin
αTubulin

B

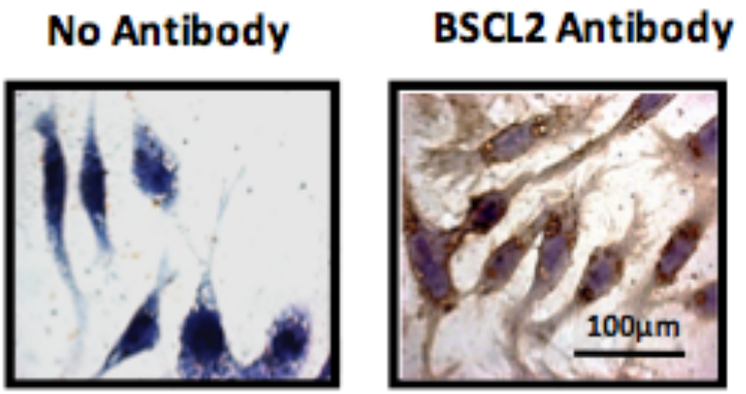
HepG2 Cells
No Antibody
BSCL2 Antibody
100µm

C

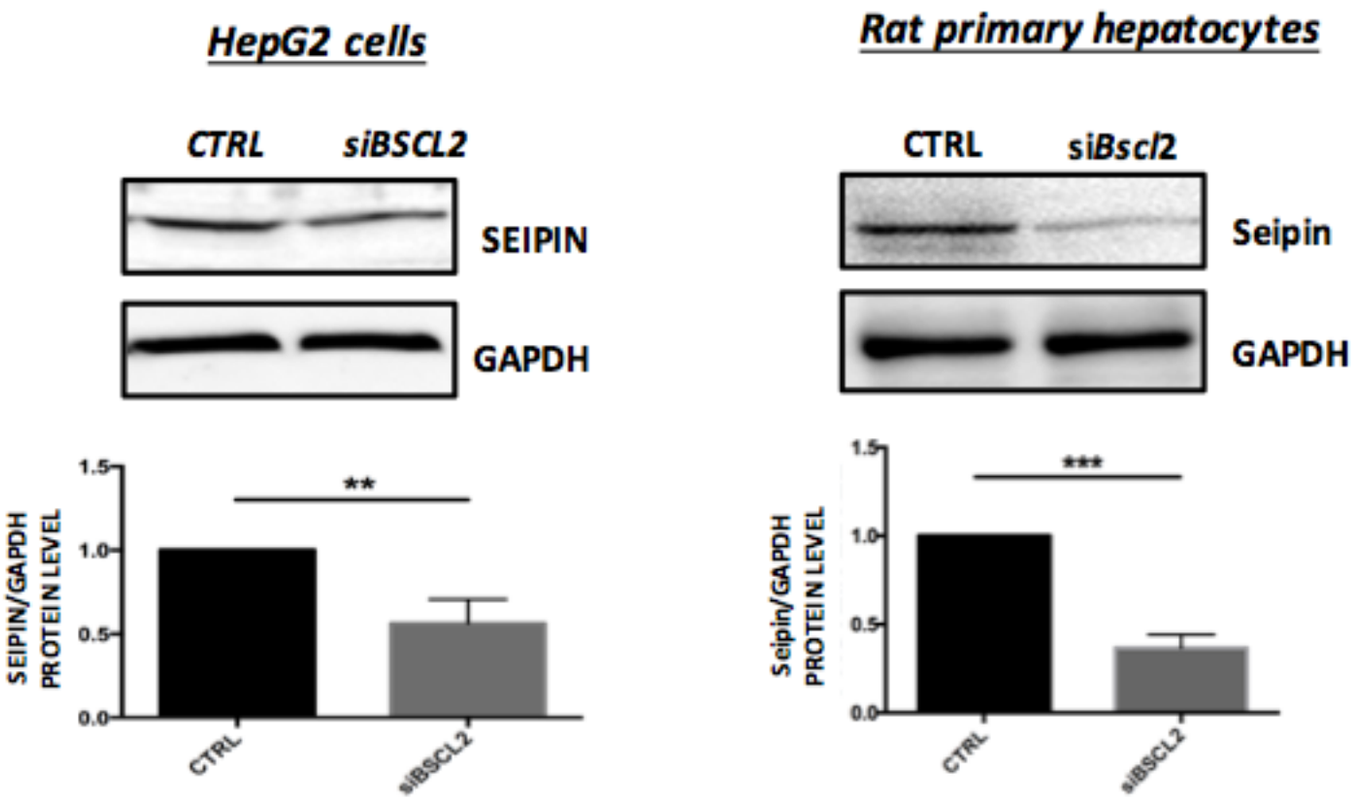
HepG2 cells
CTRL
siBSCL2
SEIPIN
GAPDH
SEIPIN/GAPDH PROTEIN LEVEL
1.5
1.0
0.5
0.0
**
CTRL
siBSCL2
Rat primary hepatocytes
CTRL
siBscl2
Seipin
GAPDH
Seipin/GAPDH PROTEIN LEVEL
1.5
1.0
0.5
0.0
***
CTRL
siBSCL2

A

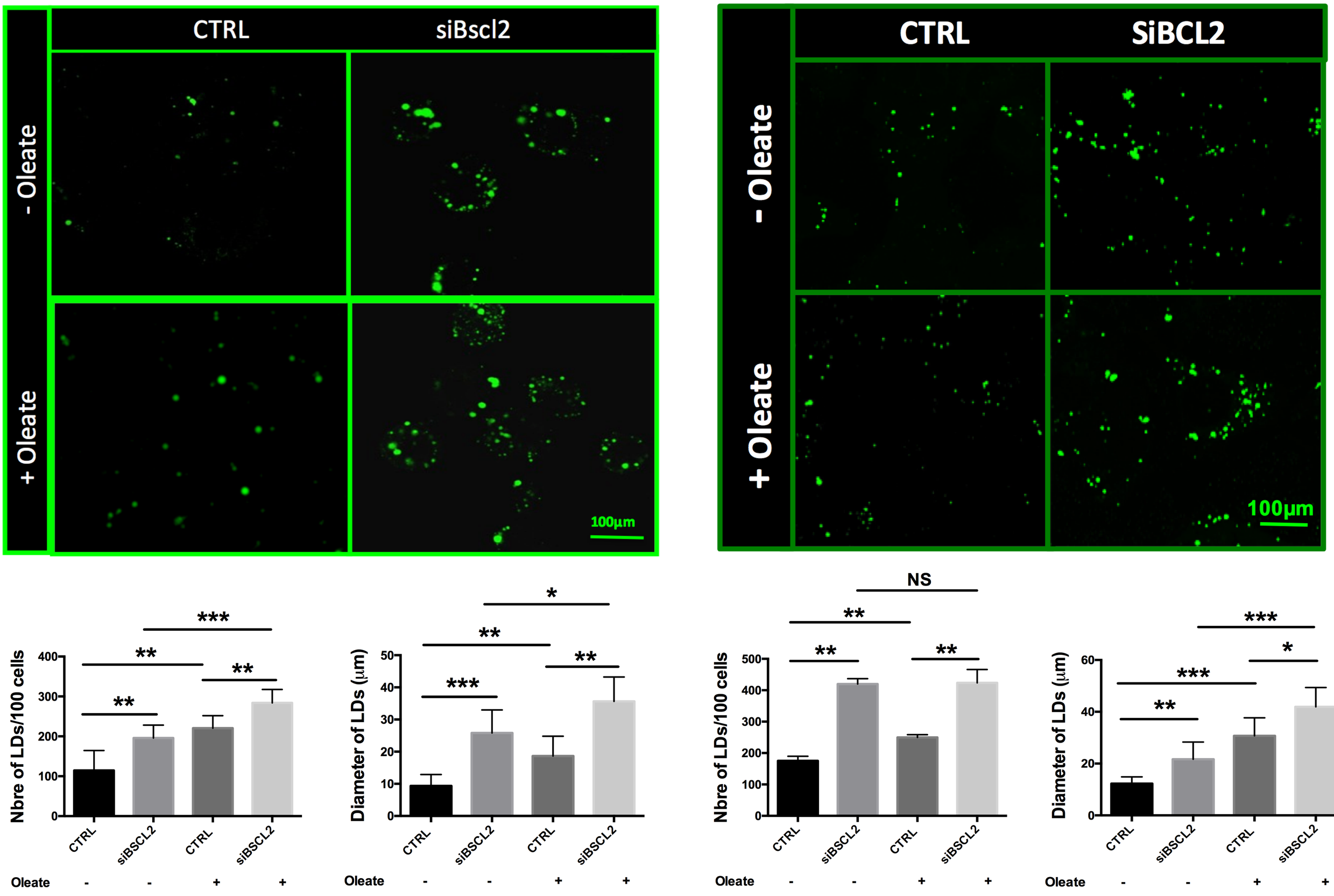
Rat primary hepatocytes
HepG2 cells
CTRL
siBscl2
SiBCL2
- Oleate
+ Oleate
100µm
Nbre of LDs/100 cells
Diameter of LDs (µm)
CTRL
siBSCL2
Oleate
NS

B

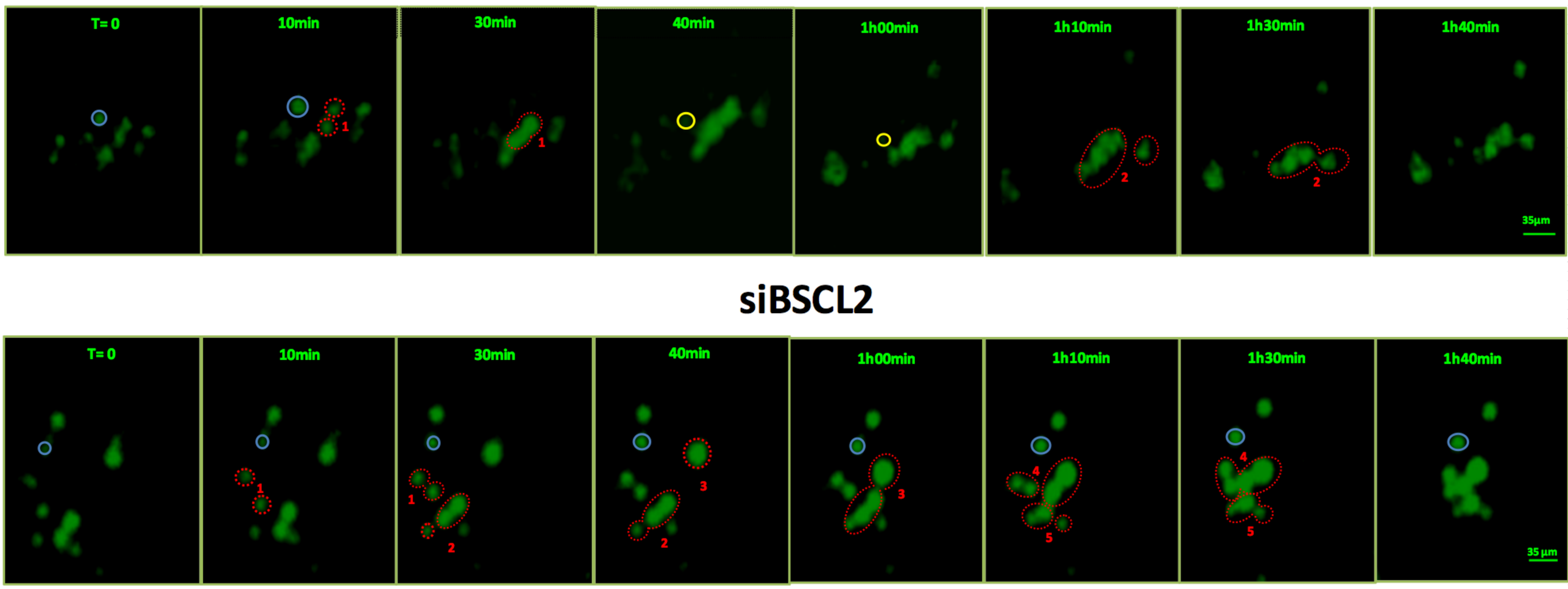
CTRL
T= 0
10min
30min
40min
1h00min
1h10min
1h30min
1h40min
35µm
siBSCL2
35 µm

HepG2 Cells

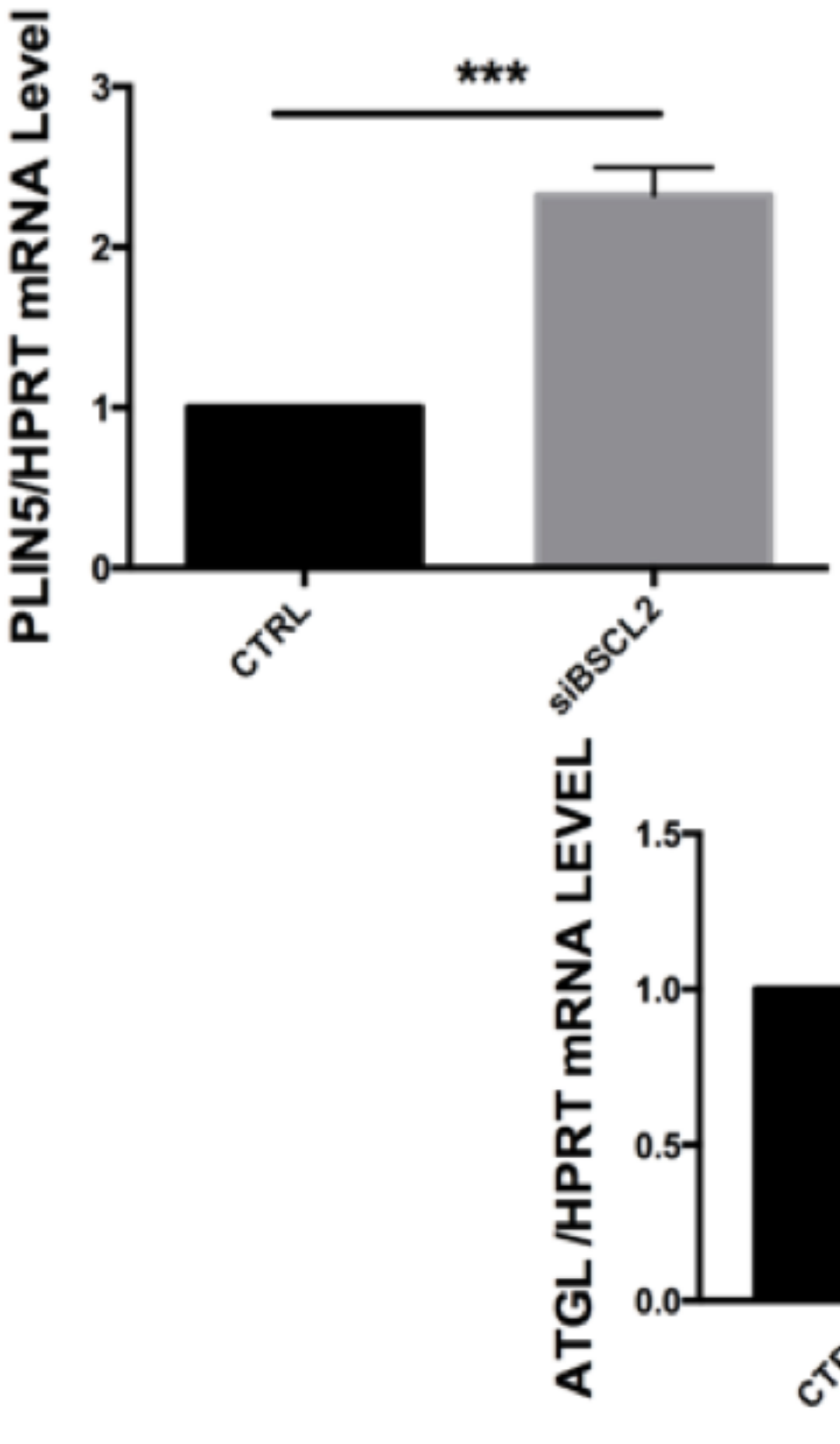

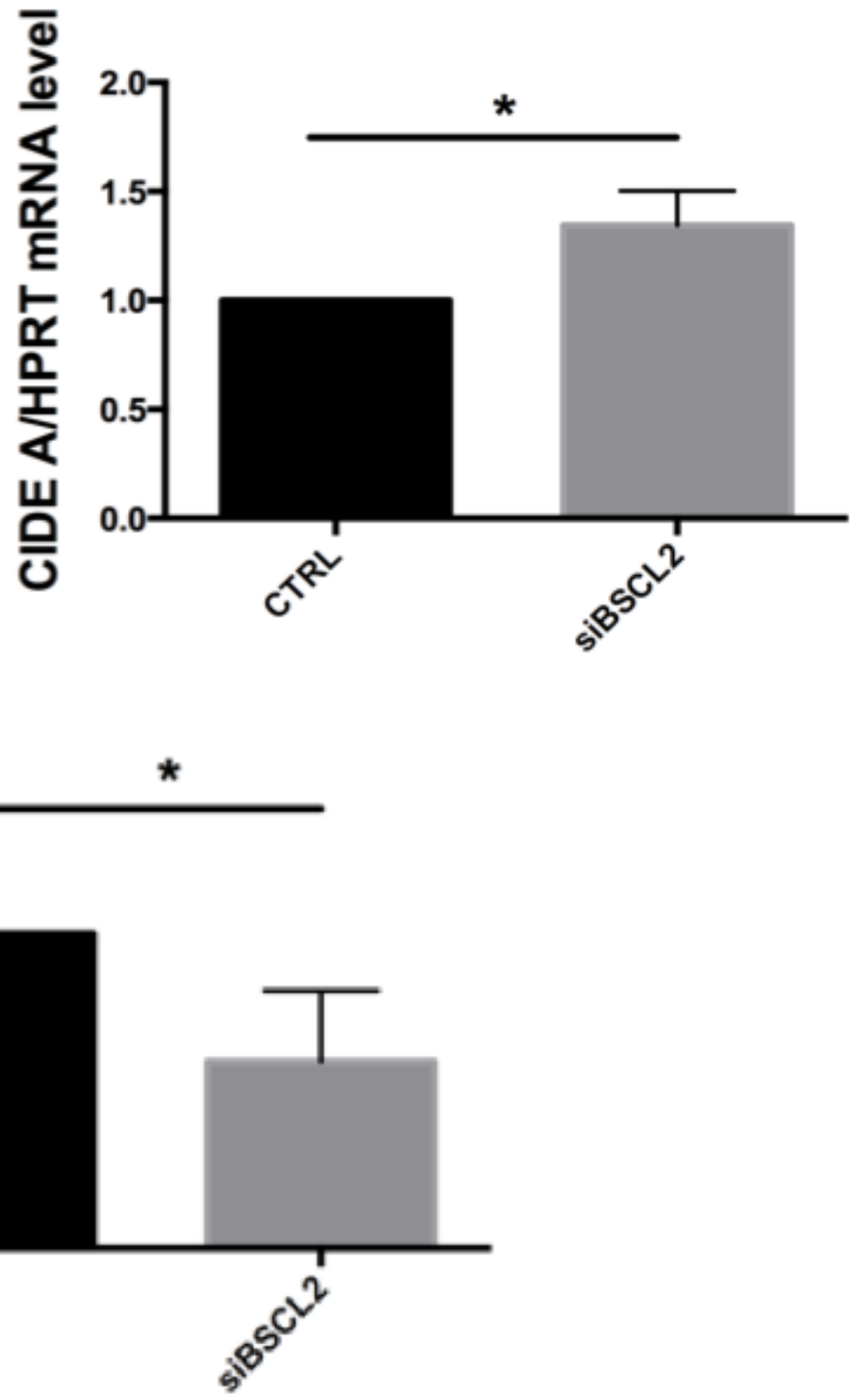

Bscl2-/- Mice

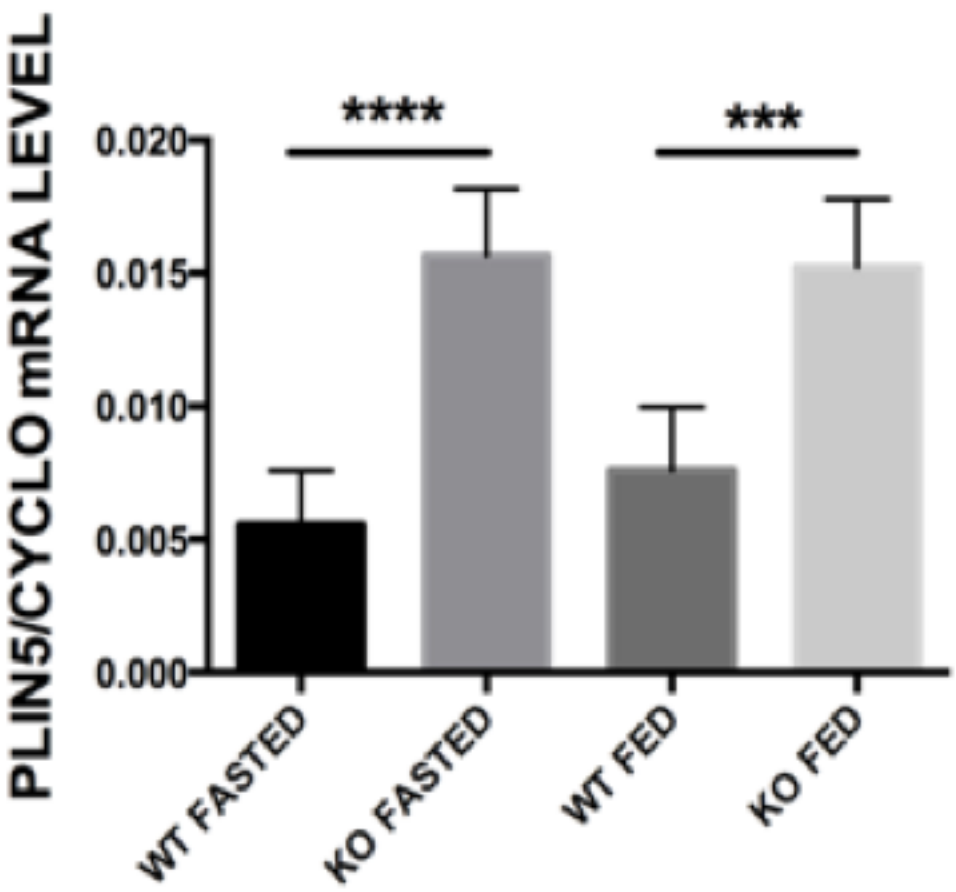

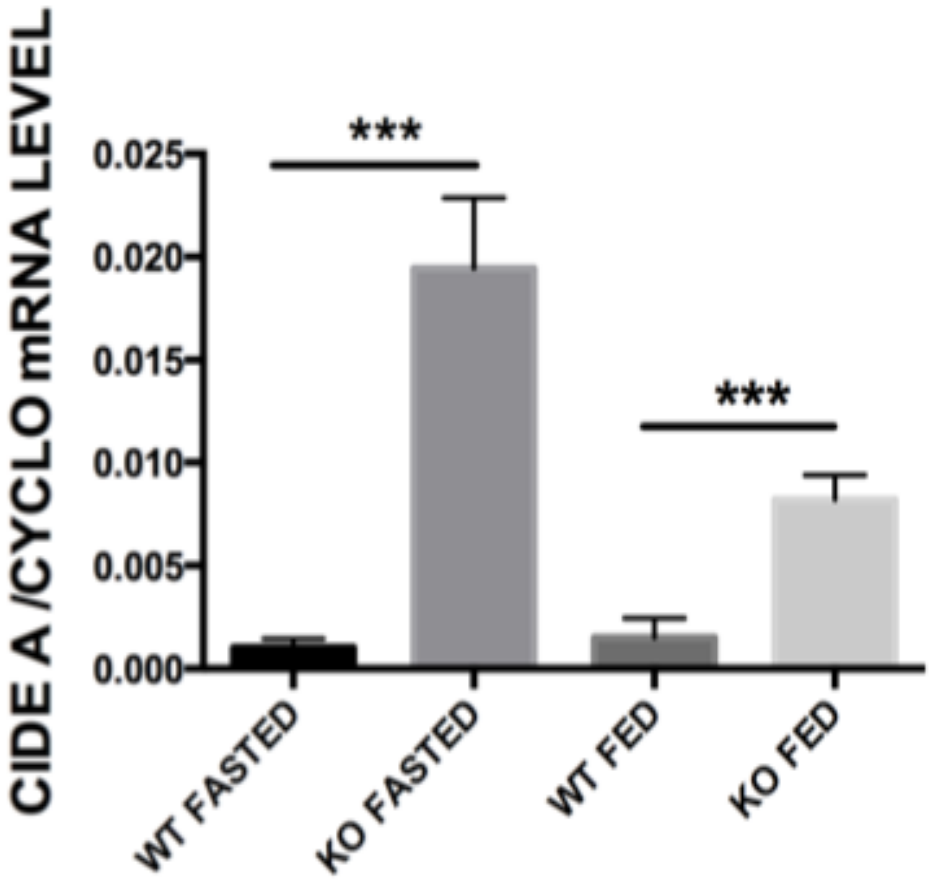

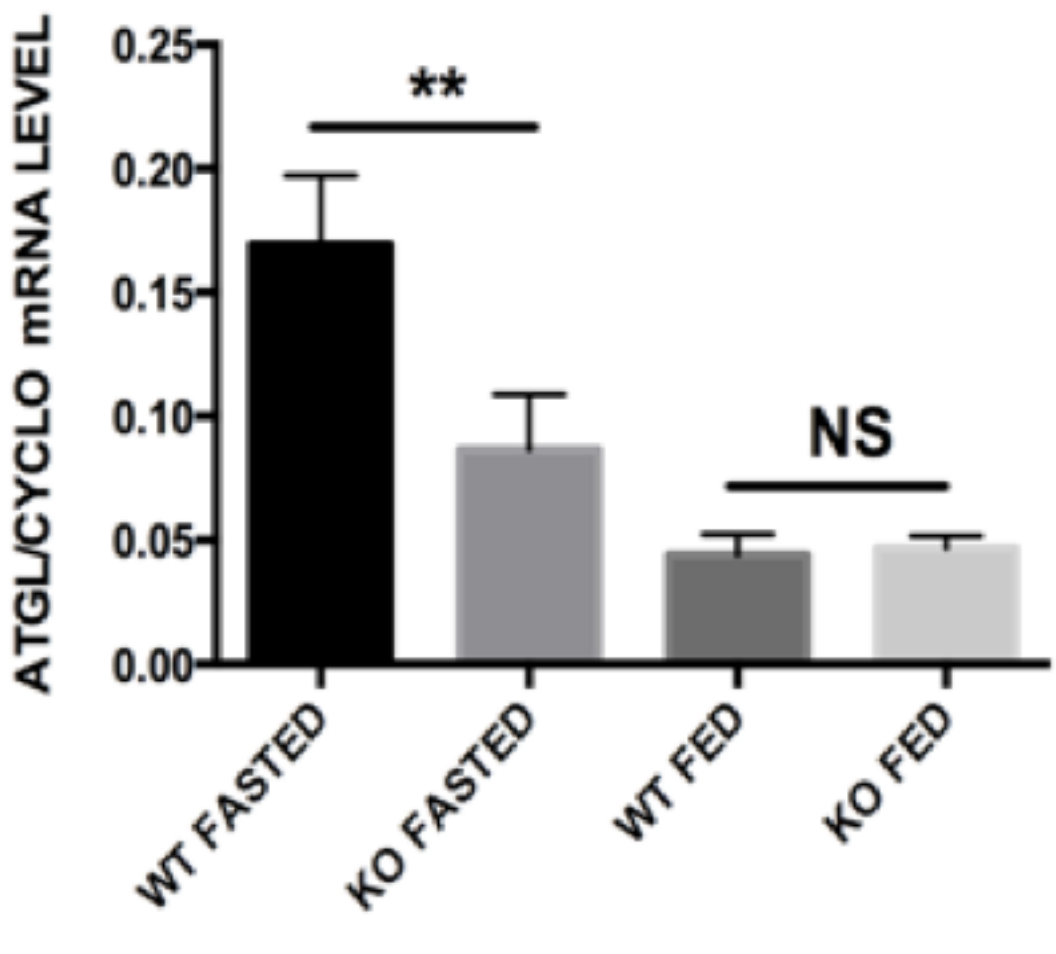

A

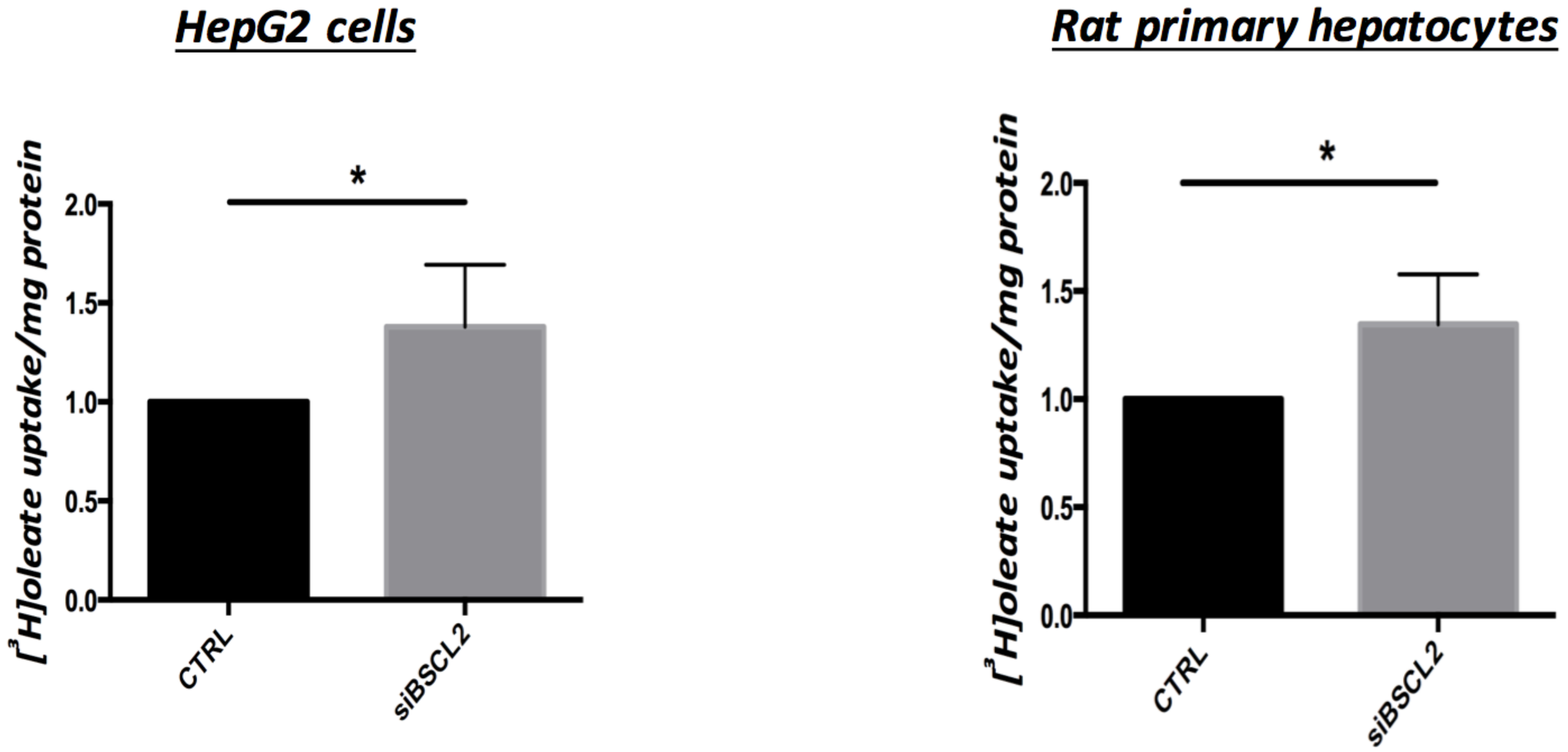
HepG2 cells
Rat primary hepatocytes
[³H]oleate uptake/mg protein
2.0
1.5
1.0
0.5
0.0
*
CTRL
siBSCL2

B

HepG2 cells
CTRL
siBSCL2
PPAR γ
GAPDH
PPARγ/GAPDH PROTEIN LEVEL
**
CD36
CD36/GAPDH PROTEIN LEVEL
***
AGPAT2
AGPAT2/GAPDH PROTEIN LEVEL
*

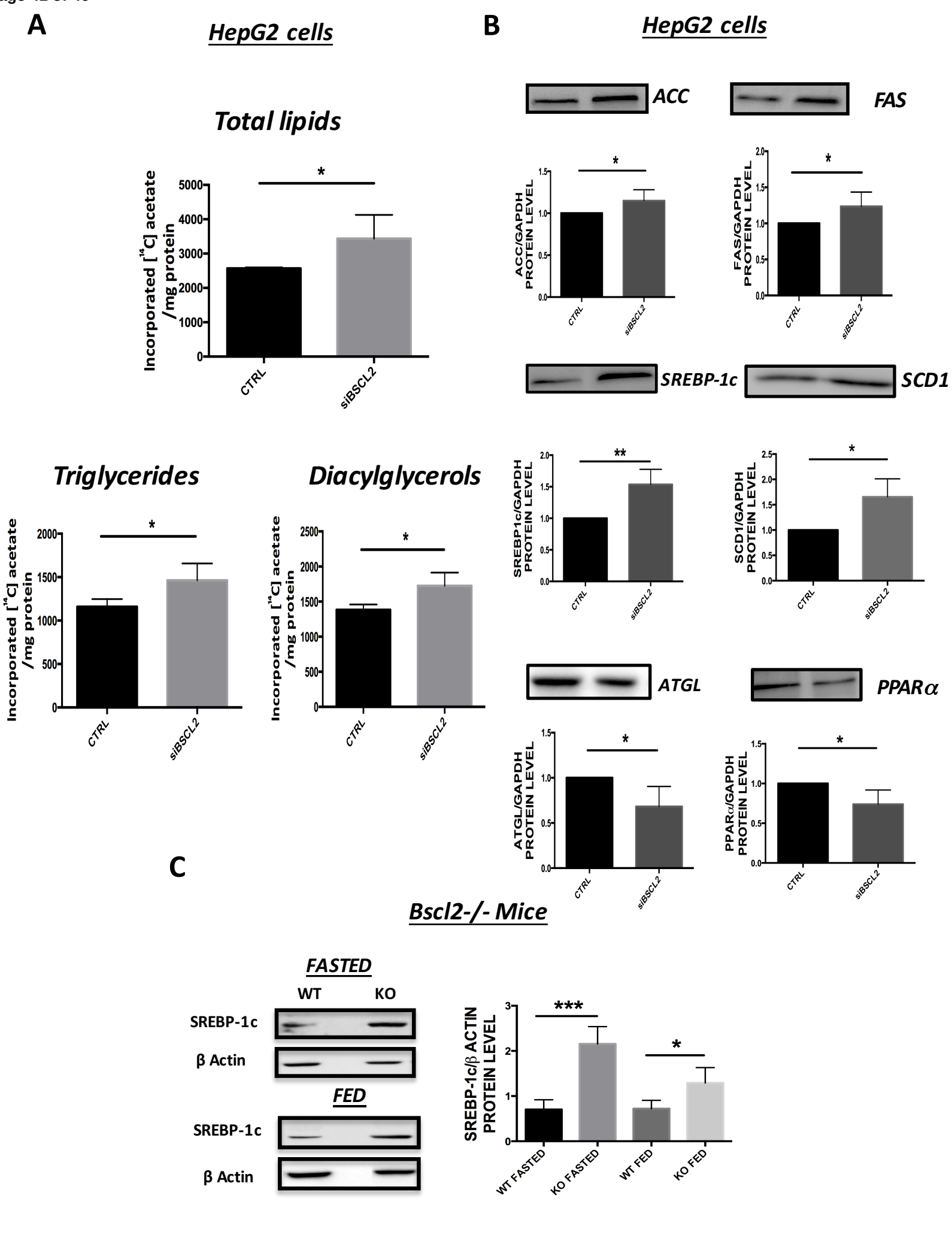
A
HepG2 cells
Total lipids
Incorporated [14C] acetate /mg protein
5000
4000
3000
2000
1000
0
*
CTRL
siBSCL2
Triglycerides
Incorporated [14C] acetate /mg protein
2000
1500
1000
500
0
*
CTRL
siBSCL2
Diacylglycerols
Incorporated [14C] acetate /mg protein
2500
2000
1500
1000
500
0
*
CTRL
siBSCL2
B
HepG2 cells
ACC
FAS
ACC/GAPDH PROTEIN LEVEL
FAS/GAPDH PROTEIN LEVEL
1.5
1.0
0.5
0.0
2.0
*
CTRL
siBSCL2
SREBP-1c
SCD1
SREBP1c/GAPDH PROTEIN LEVEL
SCD1/GAPDH PROTEIN LEVEL
2.5
**
*
ATGL
PPARα
ATGL/GAPDH PROTEIN LEVEL
PPARα/GAPDH PROTEIN LEVEL
C
Bscl2-/- Mice
FASTED
WT
KO
SREBP-1c
β Actin
FED
SREBP-1c
β Actin
SREBP-1c/β ACTIN PROTEIN LEVEL
3
2
1
0
***
*
WT FASTED
KO FASTED
WT FED
KO FED

A

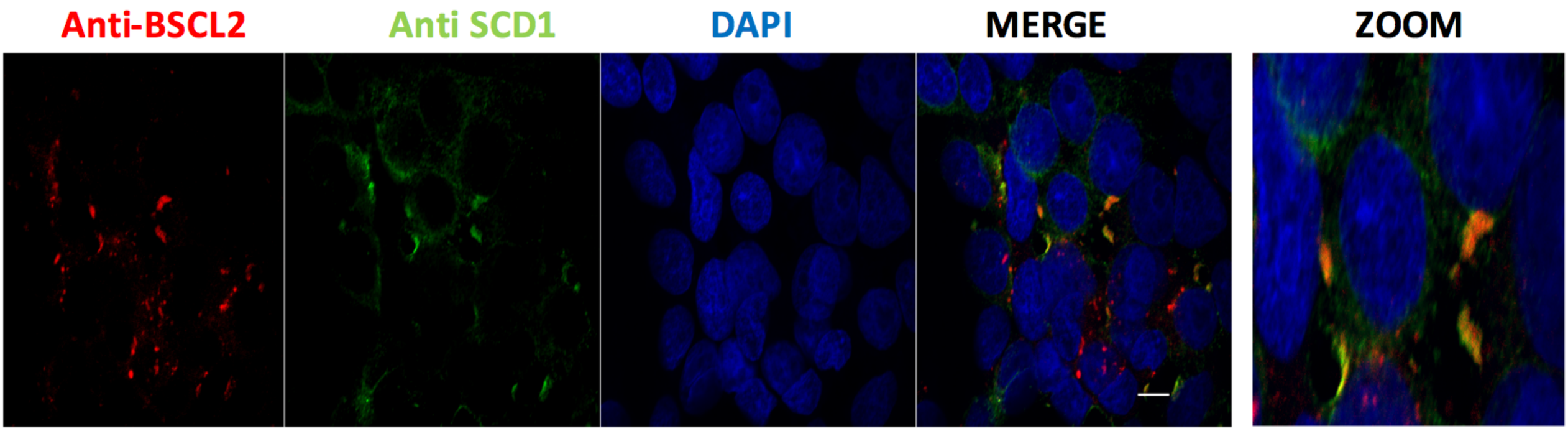
Anti-BSCL2
Anti SCD1
DAPI
MERGE
ZOOM

B

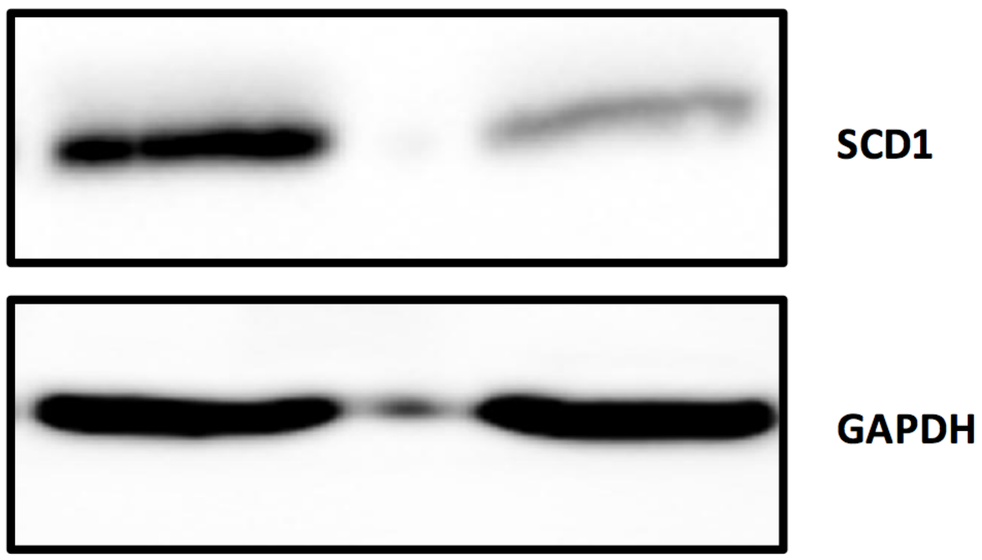
CTRL
siSCD1
SCD1
GAPDH

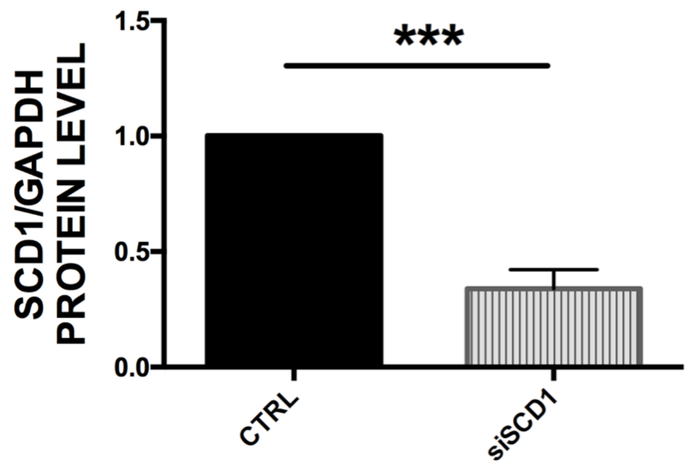
SCD1/GAPDH PROTEIN LEVEL
1.5
1.0
0.5
0.0
***
CTRL
siSCD1

C

CTRL
siSCD1
siBSCL2
siSCD1/siBSCL2
- Oleate
+ Oleate
100µm

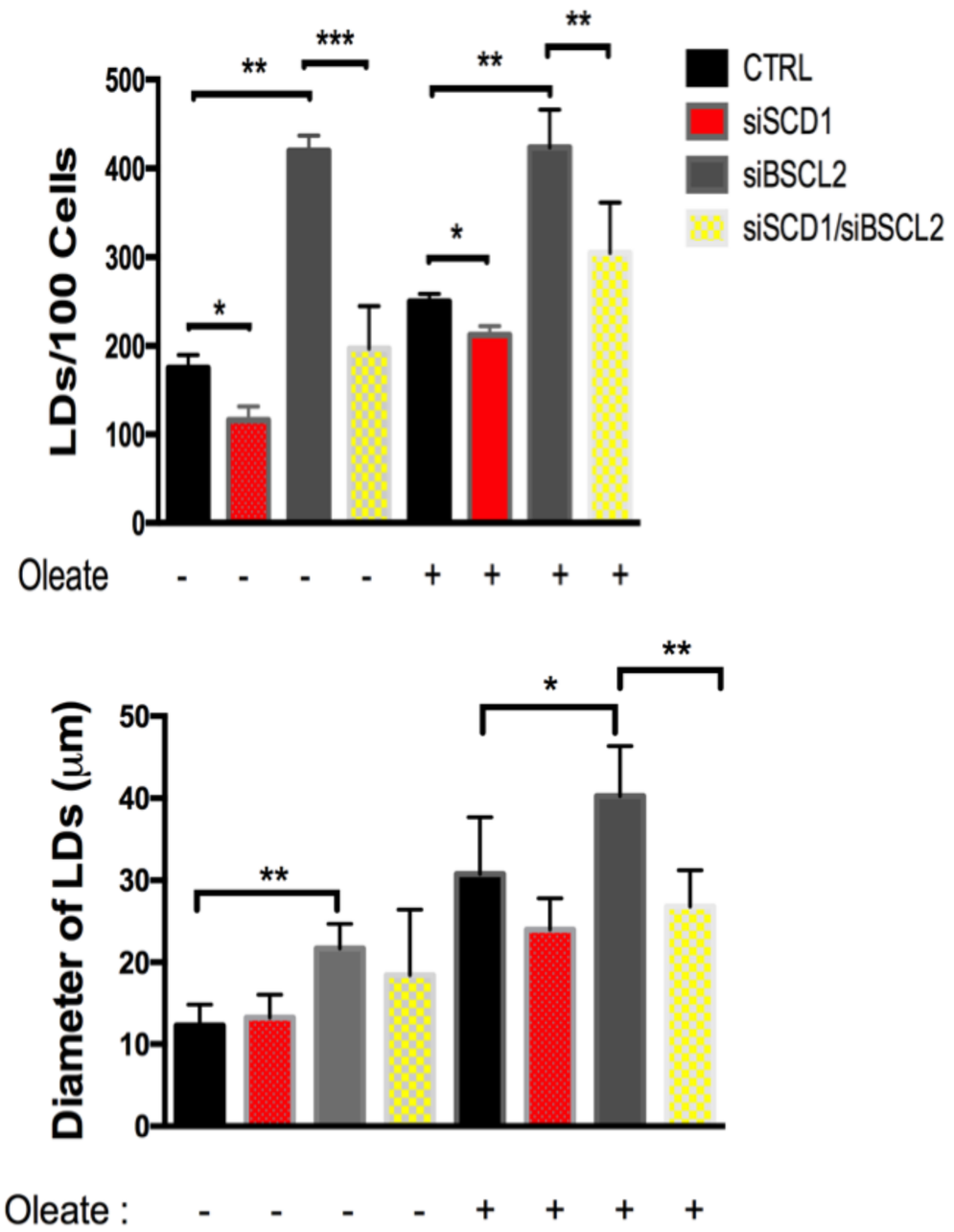
LDs/100 Cells
500
400
300
200
100
0
**
***
**
**
*
*
CTRL
siSCD1
siBSCL2
siSCD1/siBSCL2
Oleate - - - - + + + +
Diameter of LDs (µm)
50
40
30
20
10
0
**
*
**
Oleate : - - - - + + + +

D

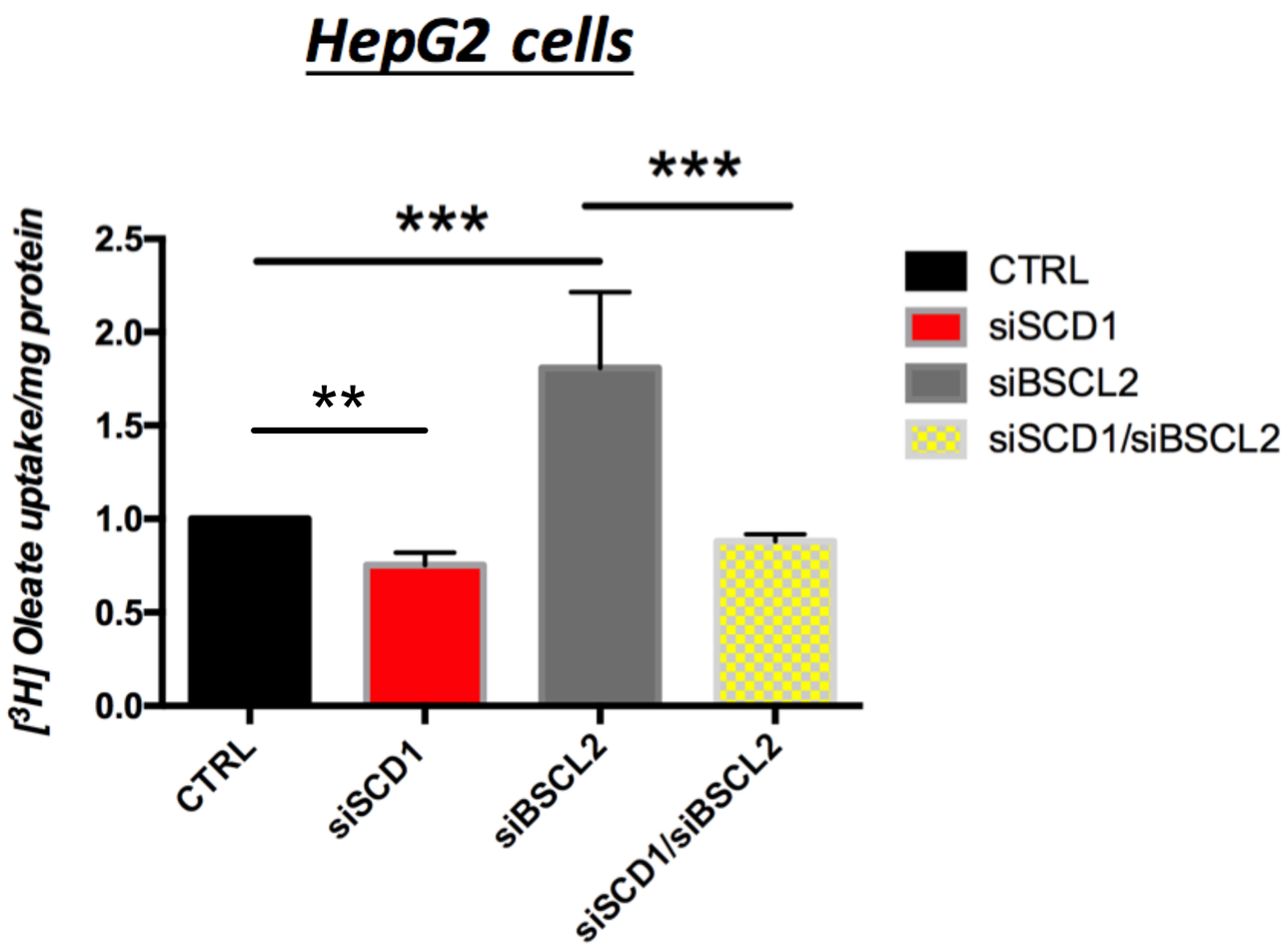
HepG2 cells
[3H] Oleate uptake/mg protein
2.5
2.0
1.5
1.0
0.5
0.0
***
***
**
CTRL
siSCD1
siBSCL2
siSCD1/siBSCL2
CTRL
siSCD1
siBSCL2
siSCD1/siBSCL2

E

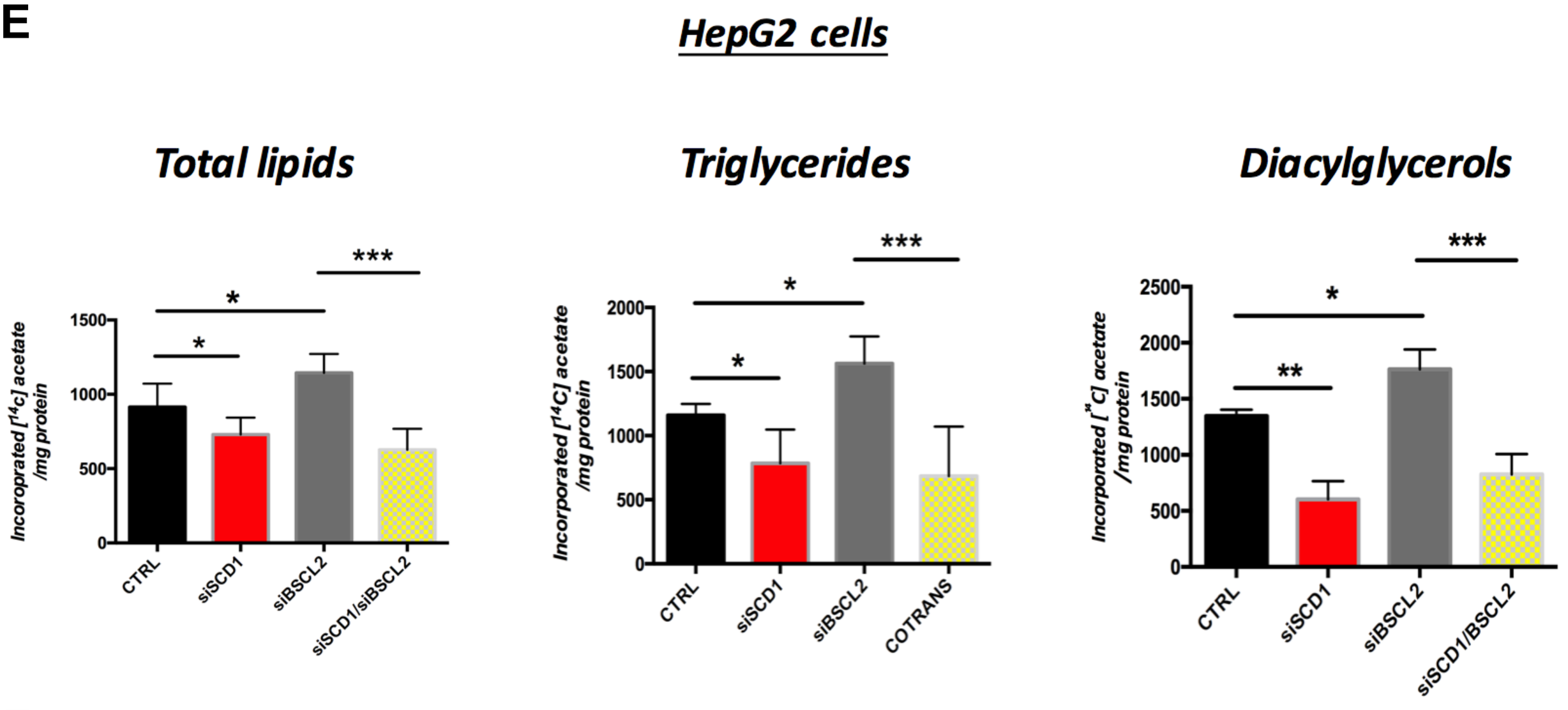
HepG2 cells
Total lipids
Incoroprated [14c] acetate /mg protein
1500
1000
500
0
*
*
***
CTRL
siSCD1
siBSCL2
siSCD1/siBSCL2
Triglycerides
Incorporated [14C] acetate /mg protein
2000
1500
1000
500
0
*
*
***
CTRL
siSCD1
siBSCL2
COTRANS
Diacylglycerols
Incorporated [14C] acetate /mg protein
2500
2000
1500
1000
500
0
*
**
***
CTRL
siSCD1
siBSCL2
siSCD1/BSCL2

F

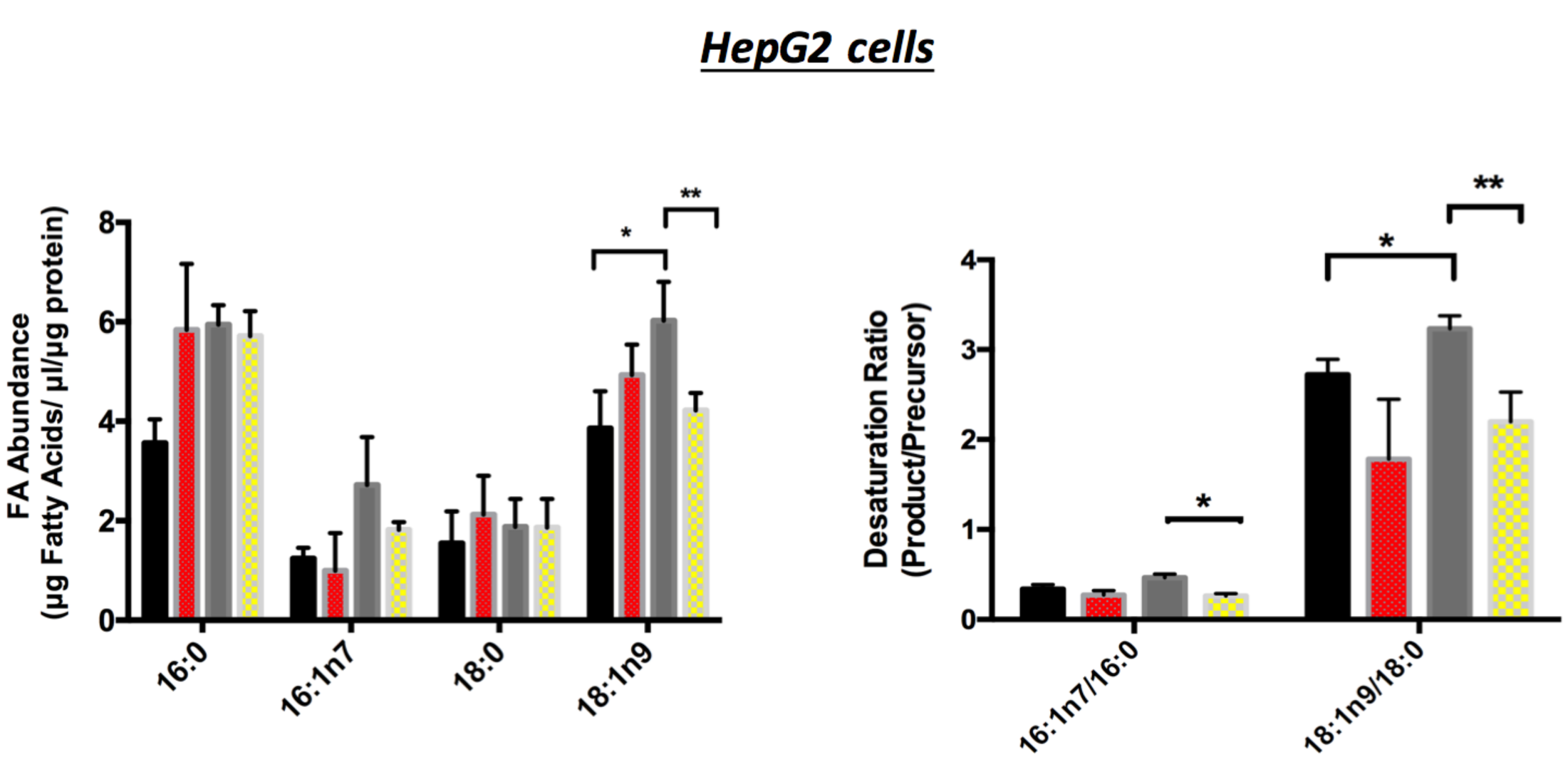
HepG2 cells
FA Abundance (µg Fatty Acids/ µl/µg protein)
8
6
4
2
0
*
**
16:0
16:1n7
18:0
18:1n9
Desaturation Ratio (Product/Precursor)
4
3
2
1
0
*
*
**
16:1n7/16:0
18:1n9/18:0

A

HepG2 cells

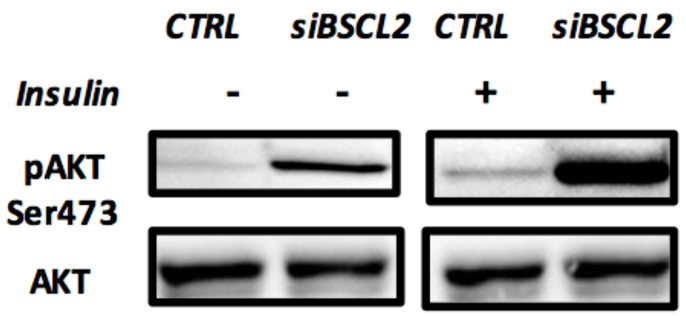

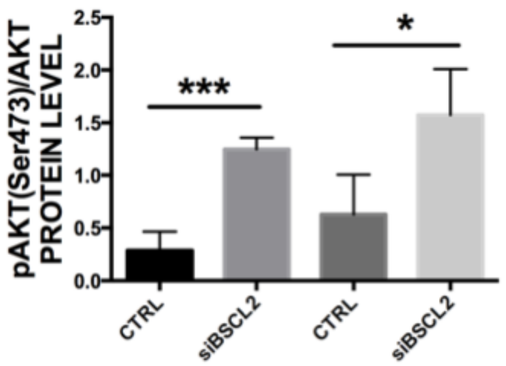

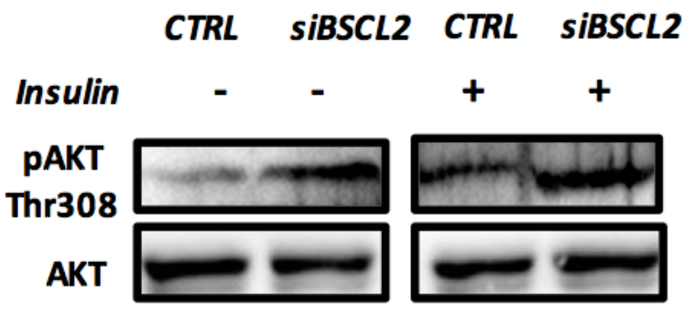

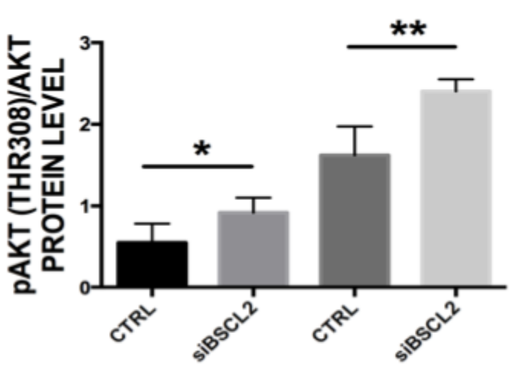

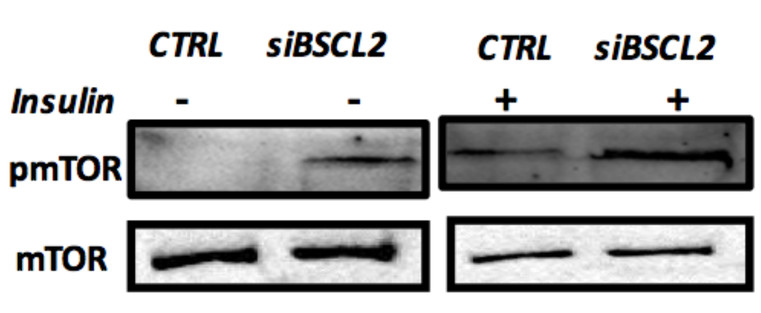

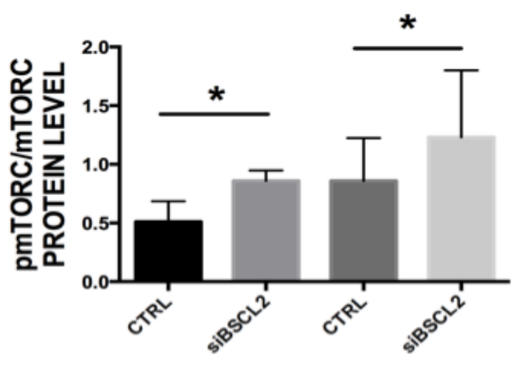

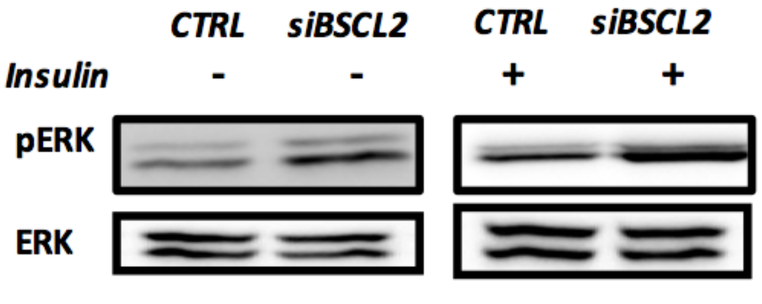

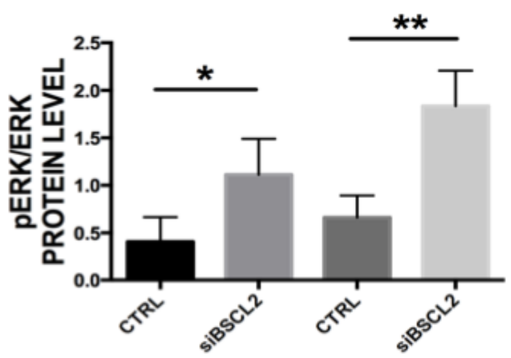

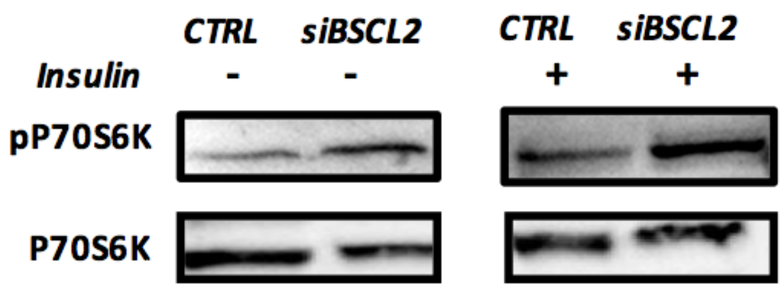

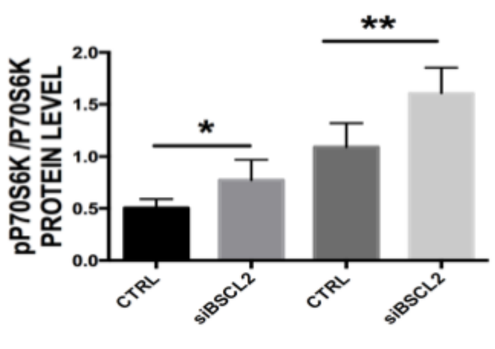

B

Bscl2-/- Mice

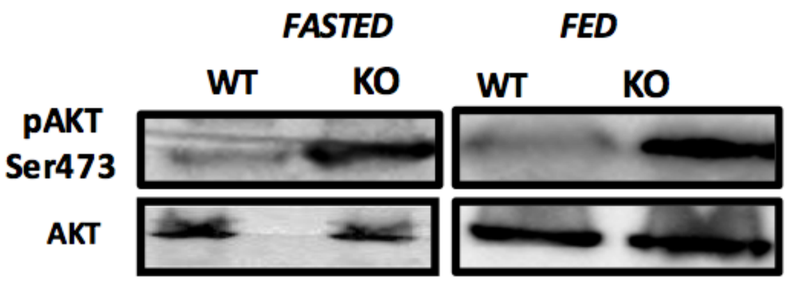

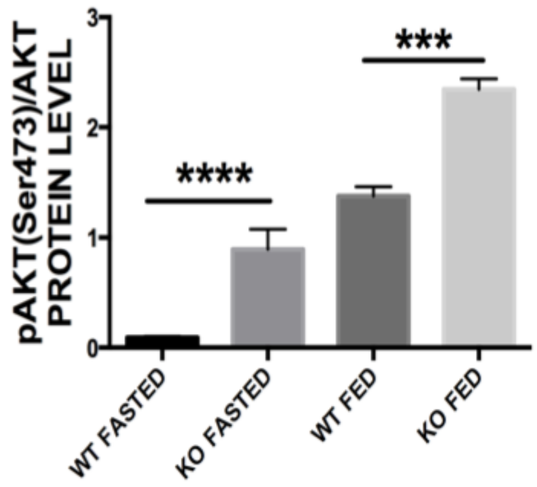

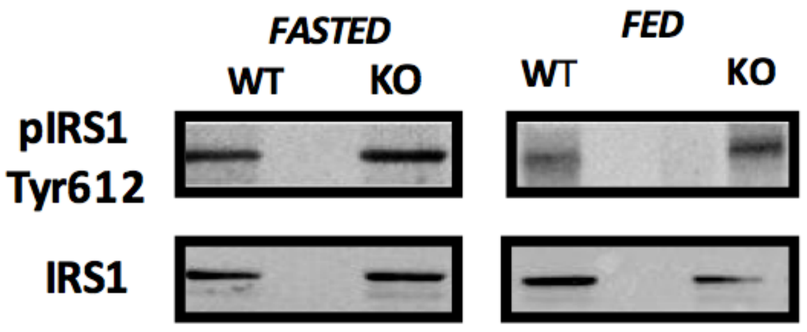

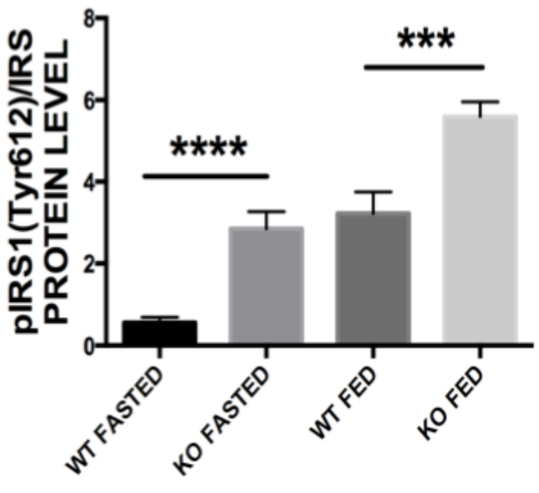

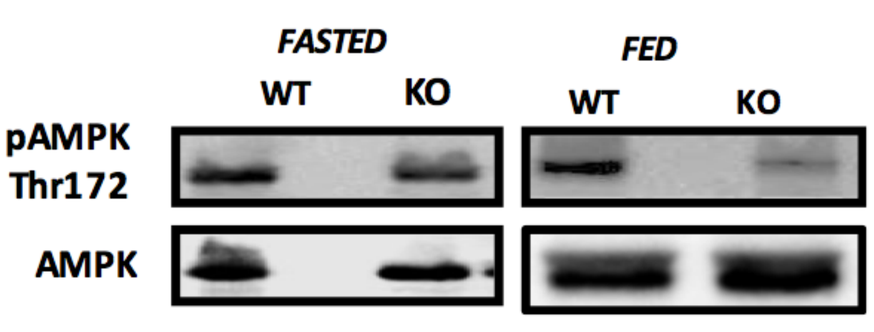

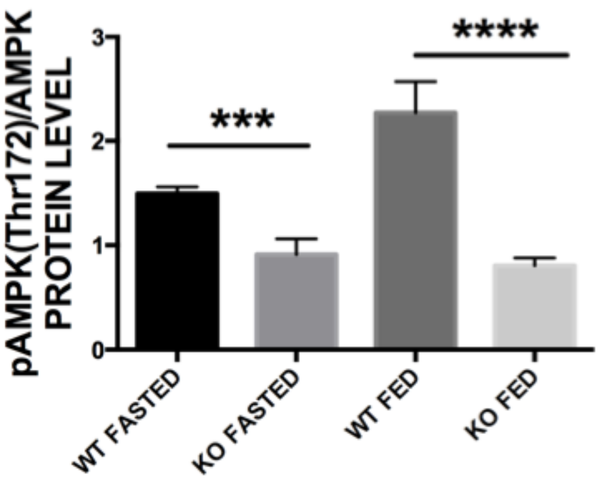

C

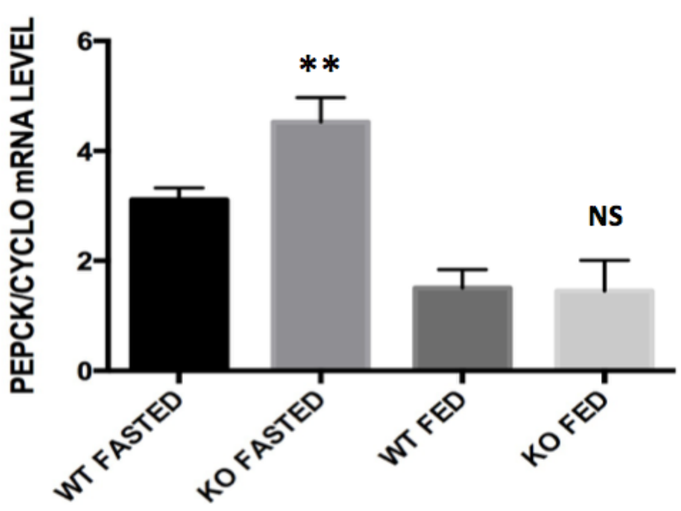

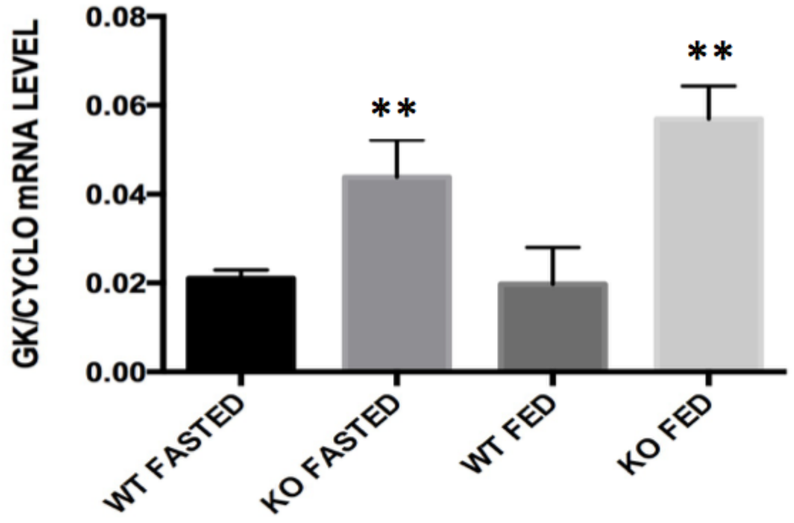

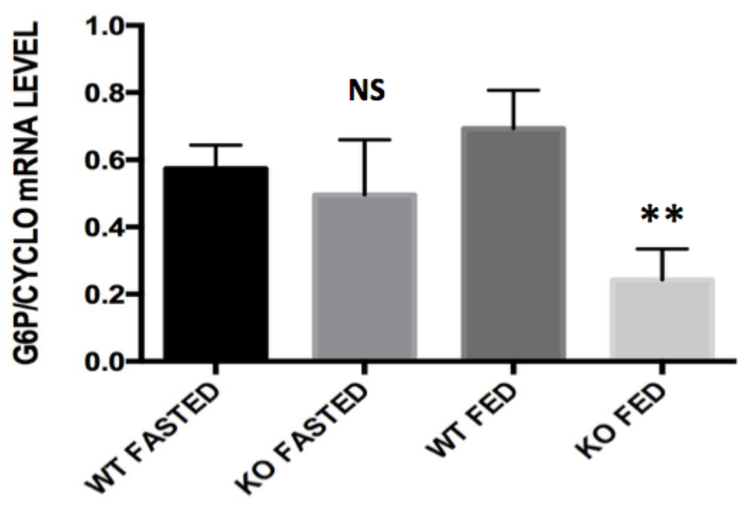

D

HepG2 cells

Fatty acids uptake

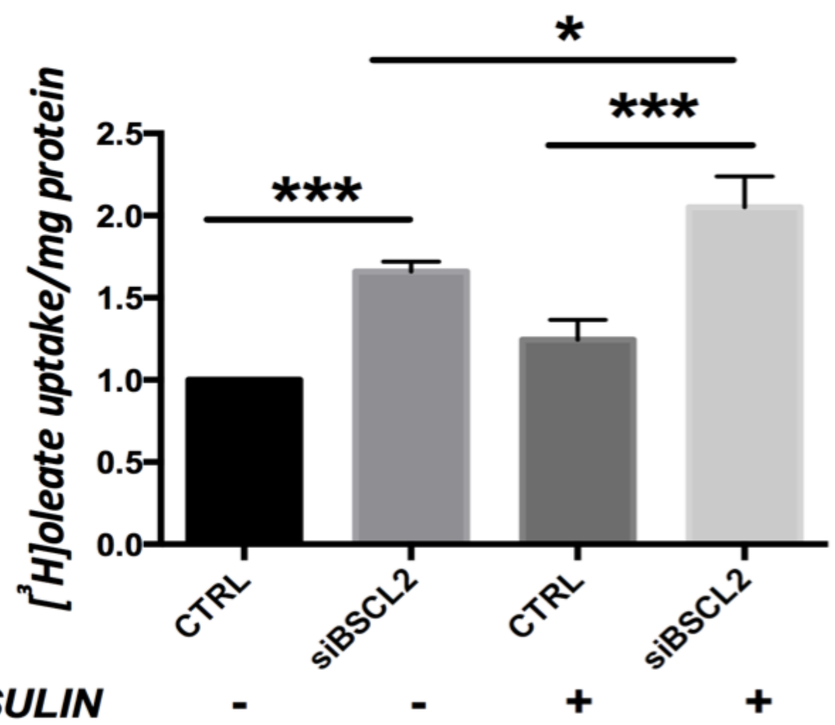

E

Total lipids

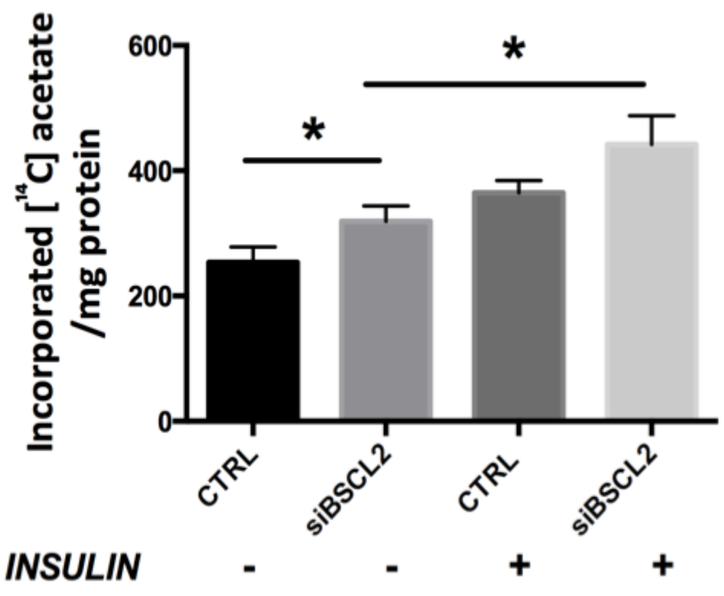

Triglycerides

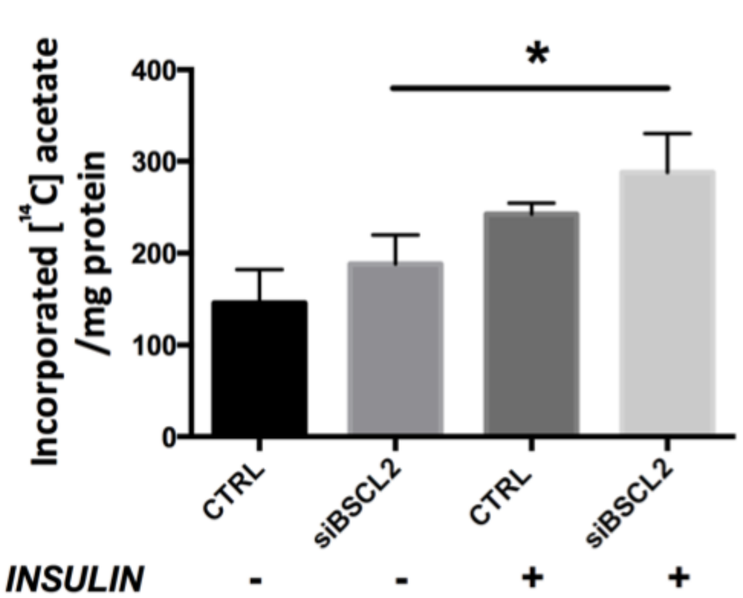

Diacylglycerols

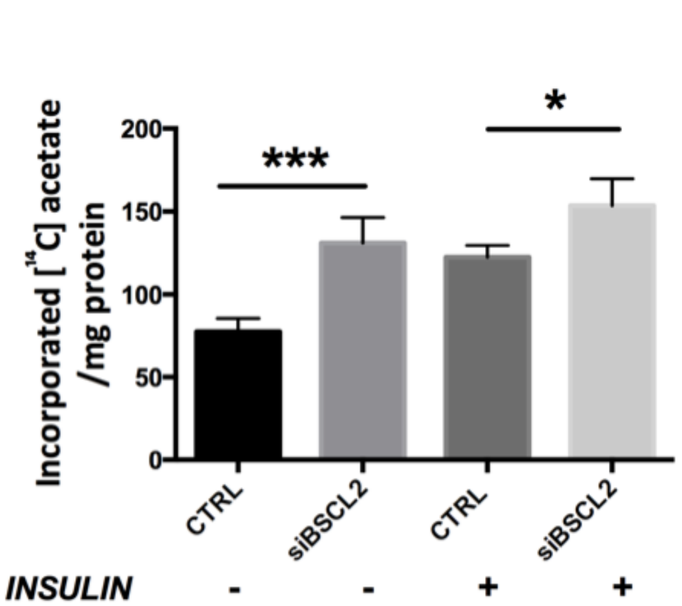

A

HepG2 cells

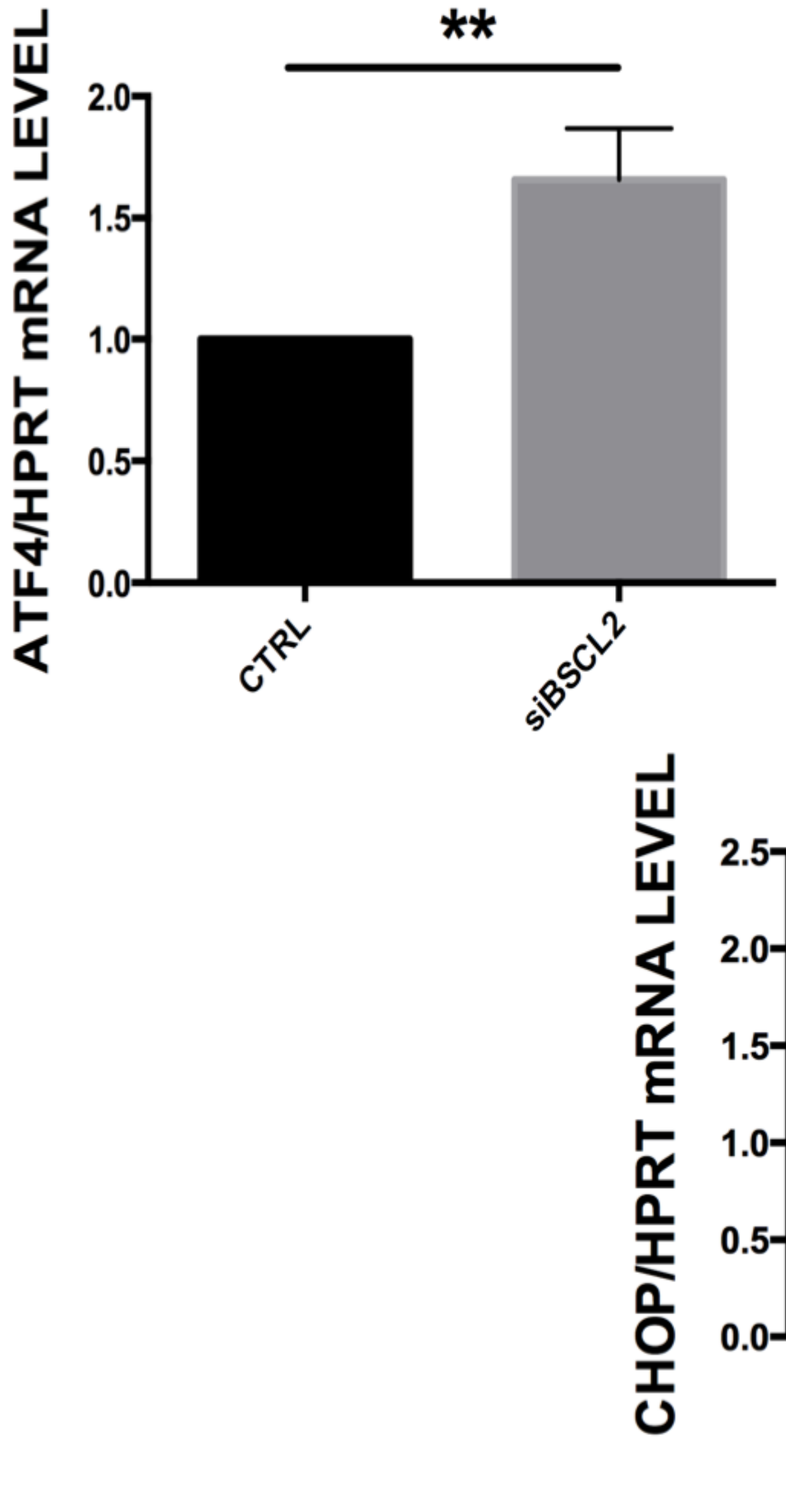

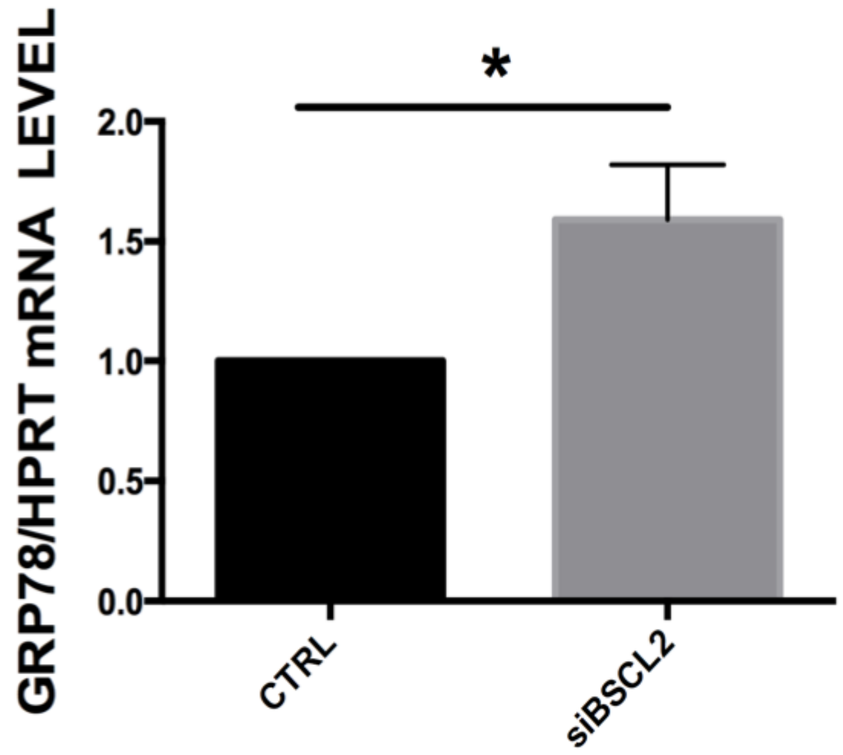

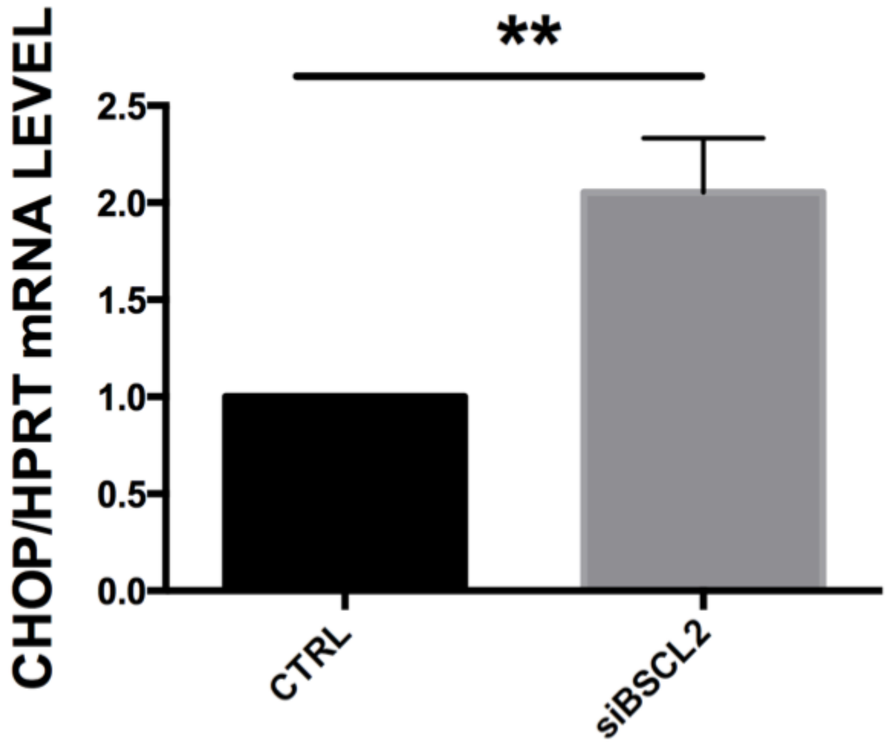

B

HepG2 cells

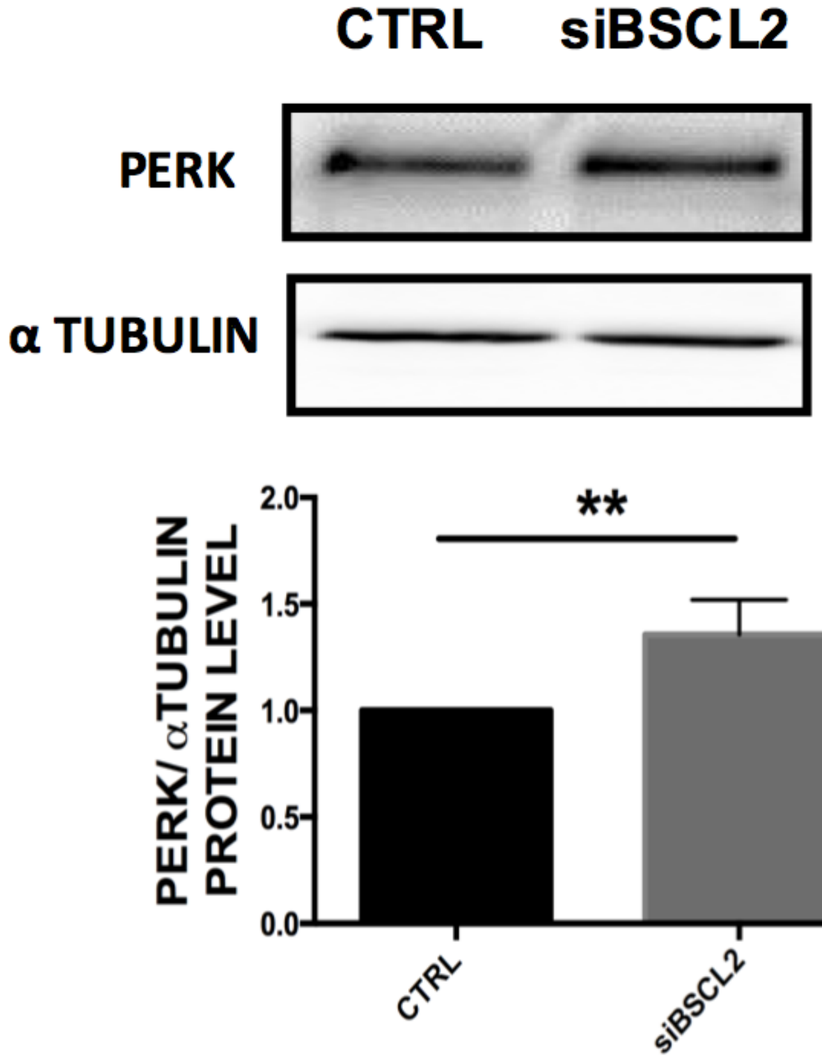

Primary hepatocytes